

Projecte de Fi de Carrera

Enginyer Industrial

Investigation of micro-architected materials with unusual combinations of stiffness and damping

Autor: Borja Auría Rasclosa

Director: Lorenzo Valdevit

Convocatòria: Setembre 2011



**Escola Tècnica Superior
d'Enginyeria Industrial de Barcelona**



Abstract

It has been known for many years that properties of individual materials can be improved by appropriately combining two materials in a composite. A stiff and a lossy material can be joined to achieve desired combinations of Young's modulus and damping coefficient, but fundamental mechanical considerations bound the achievable combinations. These bounds can be exceeded by invoking frictional loss at the interfaces between phases or by using negative stiffness elements. In this thesis we explore both concepts. In the first part, see section 2, we develop a technique to measure the loss coefficient of a micro-architected hollow-truss based material with and without polymer cores and unveil the role of the core on damping. In the second part, see section 3, we explore the possibility of developing stable systems with tunable combinations of stiffness and damping by employing electric fields to generate negative stiffness elements.





Index

ABSTRACT	1
INDEX	3
1. INTRODUCTION	5
2. MEASUREMENT OF DYNAMIC PARAMETERS OF A MICRO-ARCHITECTED MATERIALS	7
2.1. General Overview.....	7
2.1.1. Micro-architected materials	7
2.2. Manufacturing technologies	9
2.2.1. Polymeric lattice preform	9
2.2.2. Material conversion and thin-film deposition	11
2.2.3. Final product.....	11
2.3. Objective.....	14
2.4. MSA-500 Micro System Analyzer	14
2.5. Testing Methodology	15
2.6. Tested Samples	16
2.7. Procedure.....	19
2.8. Results.....	19
2.9. Processing the results.....	21
2.9.1. Viscoelastic system	21
2.9.2. Curve fitting	22
2.10. Analysis of the results	25
2.11. Conclusions.....	27
3. TUNABLE COMBINATIONS OF STIFFNESS AND DAMPING BY EMPLOYING NEGATIVE STIFFNESS ELEMENTS	28
3.1. General overview	28
3.2. Negative stiffness concept	28
3.3. Example of negative stiffness system.....	30
3.4. Capacitor: Tunable negative stiffness element.....	30
3.5. Mechanical model	31
3.6. Differential system formulation.....	34
3.6.1. Stability study.....	36
3.7. Alternative formulation of the differential system	39
3.7.1. Stability study.....	41



3.8. Real parts of the eigenvalues	41
3.9. Imaginary parts of the eigenvalues.....	43
3.10. Stability study using the central determinants graphs with Hurwitz criterion	44
3.11. Graphs of the system compliance ($1/k_{eff}$)	45
3.12. Study of the system using Laplace transform	46
3.13. Real world applications	53
3.14. Future work	54
3.15. Conclusions.....	55
4. ACKNOWLEDGMENTS	56
5. REFERENCES	57
6. ANNEX: MATHEMATICA[®] CODE	59



1. Introduction

This project is focused in the study of how developing new materials with better properties in terms of stiffness and damping. If we think about the damping and the stiffness properties of any material or composite, it is difficult to imagine that could be possible to find both properties as a relevant characteristic of a material at the same time. Either the stiffness property is high and consequently the damping property is low or the reverse, a material with a high damping will have, in general, a low stiffness. But we will investigate in this project if we can get a material, a hybrid material, that at the same time have a good combination of stiffness and damping.

This project is divided in two parts: the first one deals with a new generation of materials, hollow-truss micro-architected materials and opens a new line of investigation with non-hollow-truss micro-architected materials. Second part explores carefully a new idea based on the papers of Roderic Lakes[1] about the negative stiffness concept. How to obtain improved materials, compared with current ones, regarding stiffness and damping by using electrical capacitors as negative stiffness elements.

Referring to the first part of this thesis, we received in our department such a type of material, nano/micro structures manufactured by HRL Laboratories.

HRL Laboratories based in Malibu (CA) is the manufacturer and supplier of these micro-architected materials. A reservoir contains an appropriate photo monomer and covering it there is a photolithographic mask. An UV beam exposition through this mask within the photo monomer produces a polymerized array, the micro-architected material. A metallic electro deposition, nickel in our case, on the polymeric core and then the core removal by chemical etch give us what is called a micro-architected hollow-truss material.



During our study we propose a challenge. Why not study and compare the behavior of this micro-architected material with and without the polymer core.

This has been possible because we have commissioned a new Lab machine, the MSA-500 Micro System Analyzer. The technique this Analyzer uses is the laser-Doppler vibrometer that is a precision optical transducer for determining the vibration velocity and displacement at a measurement point.

Referring to the second part of this thesis we mix together the negative stiffness concept, the micro-architected materials and the electrical capacitors to design something that has not existed before. How we get the idea?

First of all Roderic Lakes is a brilliant professor in this field of materials and their properties and we want to experiment with his negative stiffness concept applied to the damping and stiffness properties.

Secondly, a parallel plate capacitor is an unstable system, and if we apply increasing electrical loads the attraction is increasing as well and the distance reduced. This is the behavior of a negative stiffness element. So entering tiny parallel plate capacitors within the micro-architected materials and tuning the negative stiffness by controlling the applied voltage we develop the second part of the thesis: The capacitor becomes the tunable negative stiffness element.

So we devote the second part of the thesis to know if it is possible to design materials with a higher damping and stiffness properties than current ones.



2. Measurement of dynamic parameters of a micro-architected materials

2.1. General Overview

2.1.1. Micro-architected materials

Micro-Architected Materials are a new concept in the materials' world. The revolutionary idea is to design materials with a micro-architected structure helping to increase properties like stiffness, damping or energy dissipation. This novel class of multifunctional materials could be capable of achieving new regions of Ashby's maps[2].

Until few years ago, one way to get better material properties was using composites. Mixing materials in order to get a new composite has a problem: increasing material properties like stiffness damping or energy dissipation have a maximum limit attainable. Micro-Architected materials try to beat composites limit properties using new materials design protocol, based on the synergistic interplay of optimal design algorithms, advanced manufacturing techniques and unique small-scale mechanics[3].

What is a Micro-Architected material? It is a 3D structure based on a unit-cell that is repeated along the space over and over, creating around 1mm separation between nodes. In the Figure 1 we can see a 3D simulation of the unit cell.



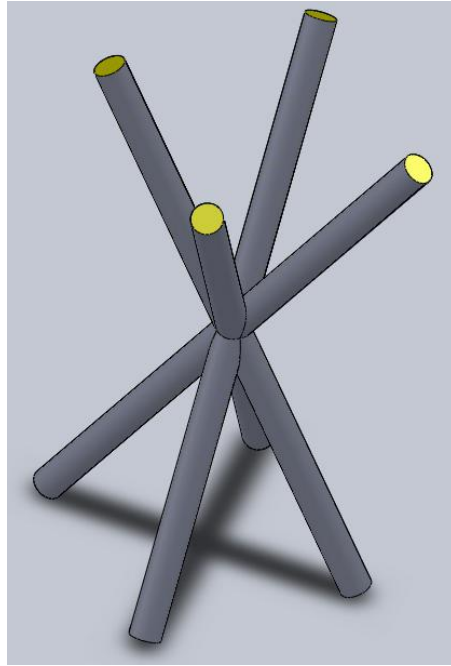


Figure 1: 3D simulation of the unit cell

The idea was to design a 3D structure based on the previous unit cell but in a micro scale creating a “solid” material with low density and high stiffness. Because of unit cells create gaps between them and they are hollow, it is possible to make a material with low density. And because of the unit-cell design, the structure helps to support higher loads or to dissipate the energy impact.

So far we explained the idea of micro-architected materials but it could never be possible without a newly manufacturing procedure capable to make this material with micro dimensions.



2.2. Manufacturing technologies

HRL Laboratories based in Malibu (CA) is the manufacturer and supplier of these micro-architected materials. But how is this new material manufactured? First of all the mold is manufactured, then a metal is electrodeposited on the mold, and eventually the mold is chemically removed.

Let's go through the manufacturing approach step by step

2.2.1. Polymeric lattice preform

Recently a new technique has been developed for building ordered open-cell polymer materials. A reservoir contains an appropriate photo monomer and covering it there is a photolithographic mask with a pattern of circular apertures, as shown in Figure 2. The mold is formed by UV exposure within the photo monomer, self-propagating polymer waveguides originate in the direction of the UV beam and polymerize together at points of intersection[3]. So you form an interconnected array of such fibers/polymer in three dimensions, and after removing the uncured monomer from the reservoir you have got a three-dimensional lattice-based open-cell polymeric material, what had call the mold, see Figure 3.

As you can imagine this new process allows us to control the architectural features of the bulk cellular material by controlling the beam angle, diameter and spatial distribution and location during fabrication. For instance, according to the pattern of the photolithographic mask you control circular apertures and orientation and the angle of the collimated incident UV light beams. So you have the ability of manufacturing truss members diameters from $\sim 10\text{ }\mu\text{m}$ to $> 1\text{ mm}$, or lattice truss angles of $\sim 50^\circ - 65^\circ$. Examples of three different types of unit cells are shown in Figure 4.



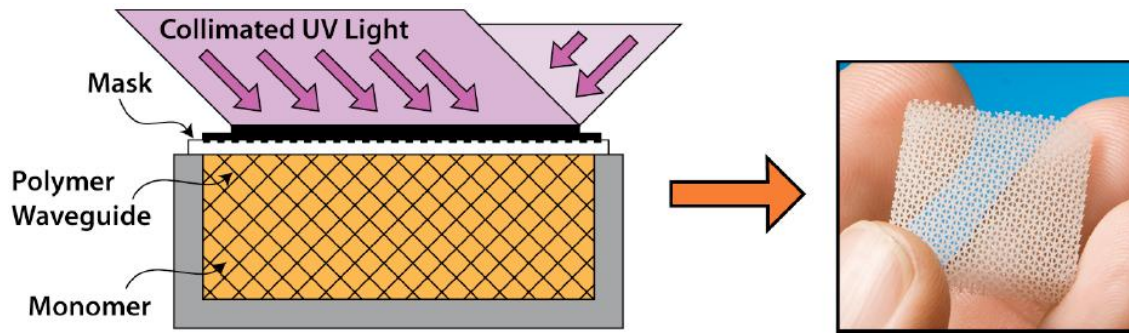


Figure 2: Schematic representation of the process used to form micro-truss structures from a self-propagating polymer waveguides and a prototypical structure formed by this process[4]

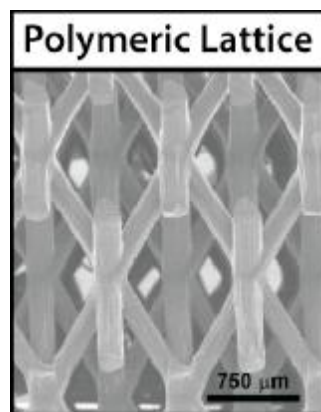


Figure 3: three-dimensional lattice-based open-cell polymeric material

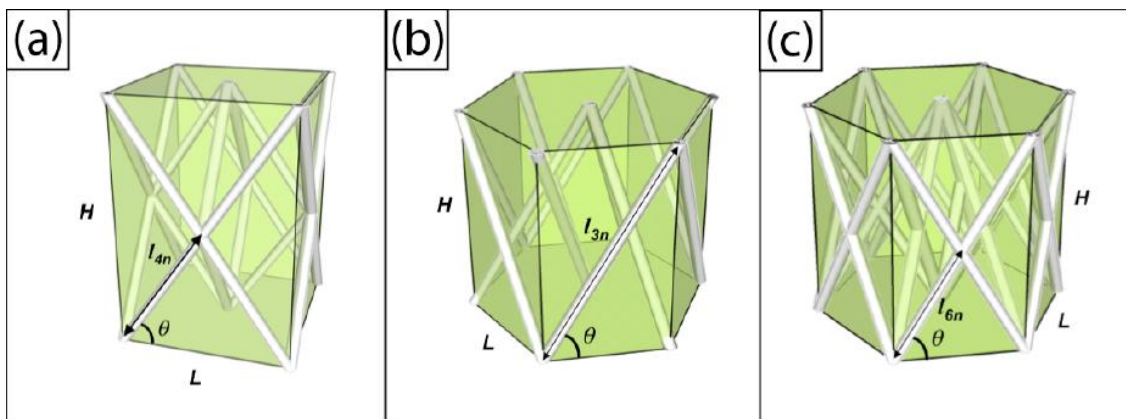


Figure 4: Examples of three different types of unit cells



2.2.2. Material conversion and thin-film deposition

So now we want to replicate the micro-architectural features of the polymer/mold. We use it as a template to apply a technique of electro deposition of a continuous metallic film, nickel in our case, on the surface of the polymer micro-lattice structure. Depending on the electro deposition time you can obtain truss diameters $\sim 10 - 100 \mu\text{m}$.

2.2.3. Final product

Now you only need to remove the polymer template. This is done with a chemical etch [5]. The open-cell periodic architecture is done and it is a hollow-tube metallic micro lattice, see Figure 5. This is the type truss we worked with.

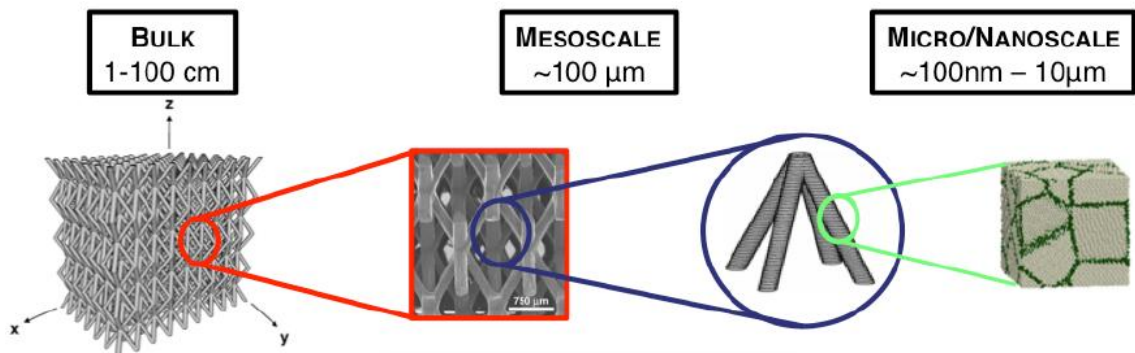


Figure 5: Dimensions of the structure

In the Figure 6 we can see an example of the micro-architected material:



Figure 6: Hollow-truss micro-architected material



This picture is an example of a hollow-truss micro-architected material, when the polymer mold had been removed.

We were able to see with more details the nickel structure using an electronic microscope. In the following figures there are examples of the hollow-truss. In these images we can see details of the structure and we can have an idea of the geometric dimensions. The polymer mold has been removed in these samples.

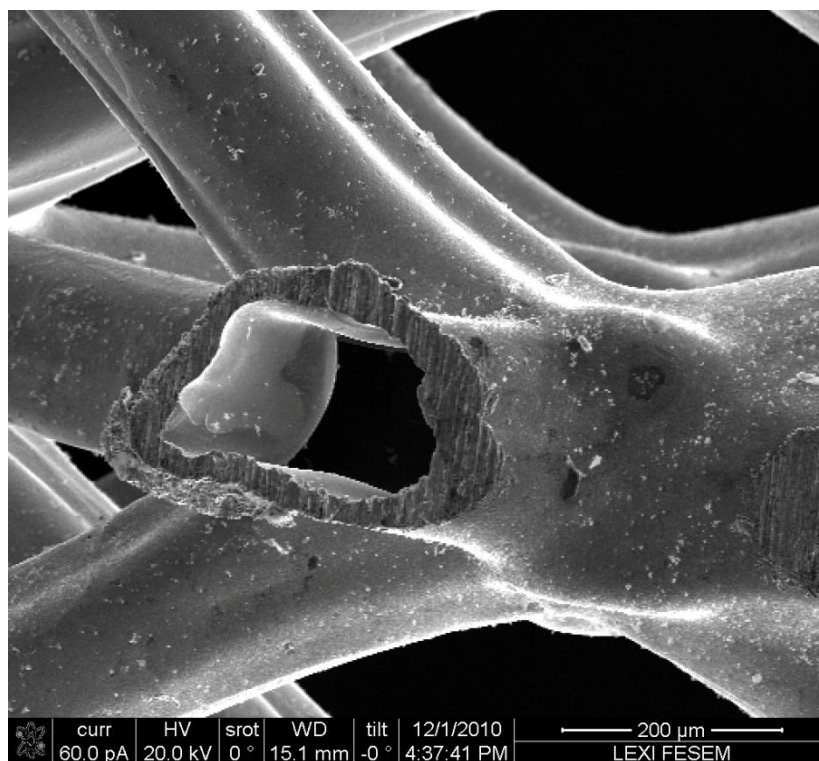


Figure 7: SEM image courtesy of Anna Torrents



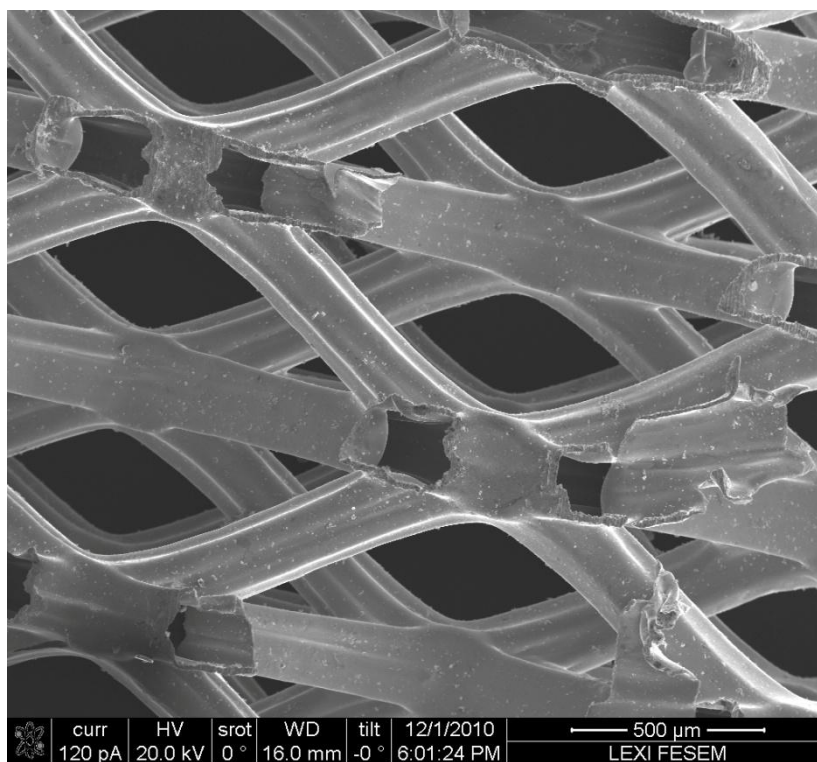


Figure 8: SEM image courtesy of Anna Torrents

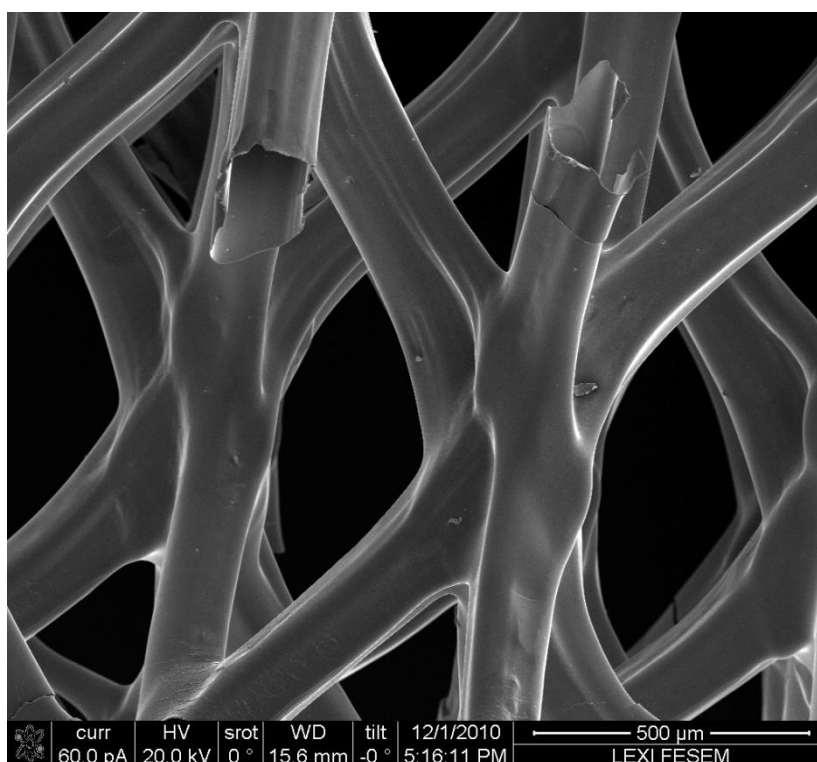


Figure 9: SEM image courtesy of Anna Torrents



2.3. Objective

HRL laboratories started to manufacture micro-architected materials with hollow-truss. They used polymer mold only as a step for a final goal, namely to have a nickel hollow structure. The first idea was to get a material with the lowest density possible, so they decided to dissolve the polymer.

In our department we wanted to study if it could be useful to keep the polymer inside for some applications. We thought that the damping could be higher with the polymer inside the truss.

In order to do a first test to calculate the damping coefficient of some samples, we decided to use the new Micro Systems Analyzer MSA-500, a new machine in our laboratory that was able to measure vibrations with very high precision.

So HRL laboratories sent to us a sample without removing the polymer to be investigated.

2.4. MSA-500 Micro System Analyzer

In the following illustration, Figure 10, we can see the MSA-500 Micro System Analyzer[6]:



Figure 10: MSA-500 Micro System Analyzer[6]



This technique uses the laser-Doppler vibrometer that is a precision optical transducer for determining the vibration velocity and displacement at a measurement point. It works by sensing the frequency shift of back scattered light from a moving surface. The object scatters or reflects light from the laser beam and the Doppler frequency shift is used to measure the component of velocity along the axis of the laser beam.

2.5. Testing Methodology

We developed a test for these micro-architected materials trying to find vibrational modes and loss factors at microscopic scale in the frequency range of 0.1 Hz - 20 kHz in order to get information about the damping coefficient of the materials.

The procedure for conducting the test was to use 4 samples of the micro-architected material, each sample with different properties:

- 4 samples tested:
 - 2 beams :
 - One with polymer
 - One without polymer
 - 2 plates:
 - One with polymer
 - One without polymer

Just to understand what is the meaning of a sample with or without polymer we must remember the manufacturing procedure. A series of beams, UV light, generate the polymeric 3D micro-architected material, truss. Then the micro structure is coated by a metal, nickel in this case, with different times of deposition. In our case samples of 8 hours nickel deposition time micro-architected materials were used.



The manufacturer dissolved the polymer as a default way, but we received samples including the polymer.

These four samples were tested using the MSA-500 Micro System Analyzer developed by Polytec Company. This equipment allowed us to calculate vibrational modes of the different samples. Using scanning laser-Doppler vibrometry allowed us non-contact measurements in real time for the characterization of out-of-plane vibrational behavior and for determining the vibration velocity and displacement at any sample point.

We needed to excite our samples with different frequencies in a wide range trying to find the vibrational modes. In order to do that, we used a high definition speaker increasing the frequency in 0.1 Hz intervals until 20 kHz.

2.6. Tested Samples

For the test we used 4 samples with different geometries and properties. We received from HRL Laboratories samples roughly of 3 x 2 x 1 cm. Using these pieces of material we prepared each sample. We had to cut them using a diamond blade. We decided to use two type of samples (one with polymer and other without polymer) to compare if the polymer inside the structure was important computing the damping coefficient of the system. For each type of sample we cut two types of geometries trying to avoid some possible errors due to lack of accuracy on the dimensions. You can see in Figures 11 to 14 the prepared samples, dimensions of which are for the beam type 20 mm x 2 mm x 2.5 mm roughly and for the plate type 20 mm x 2 mm x 7 mm roughly. In these figures we indicated the point of measurement where we focused the laser of the MSA-500 to calculate the vibration of the sample. We chose the extreme point of the sample because supposedly the oscillation amplitude was larger.



- Beam with polymer:

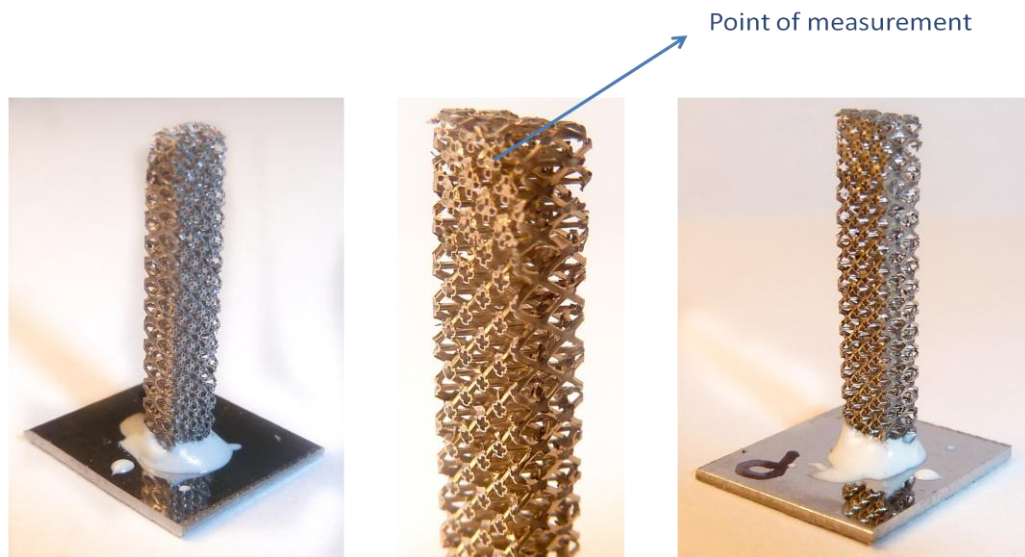


Figure 11: Beam with polymer

- Beam without polymer

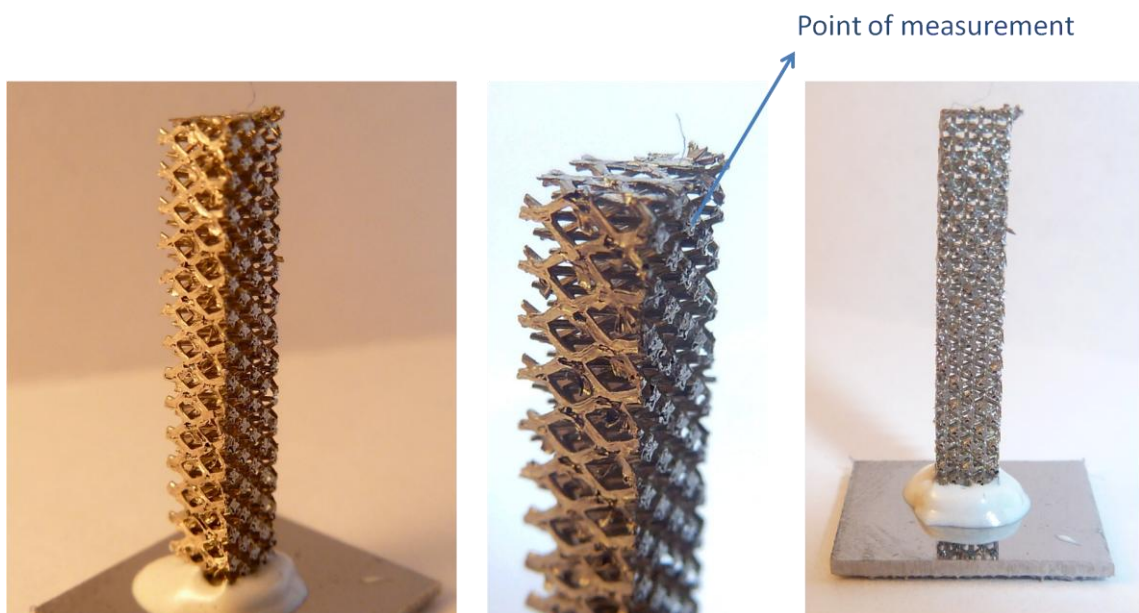


Figure 12: Beam without polymer



- Plate with polymer

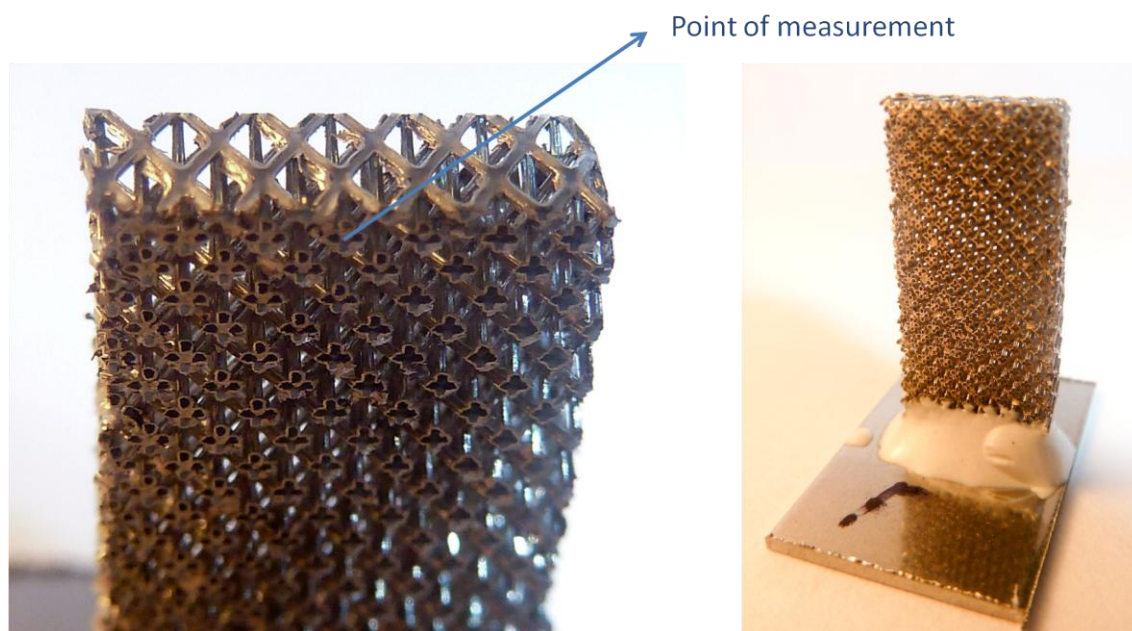


Figure 13: Plate with polymer

- Plate without polymer

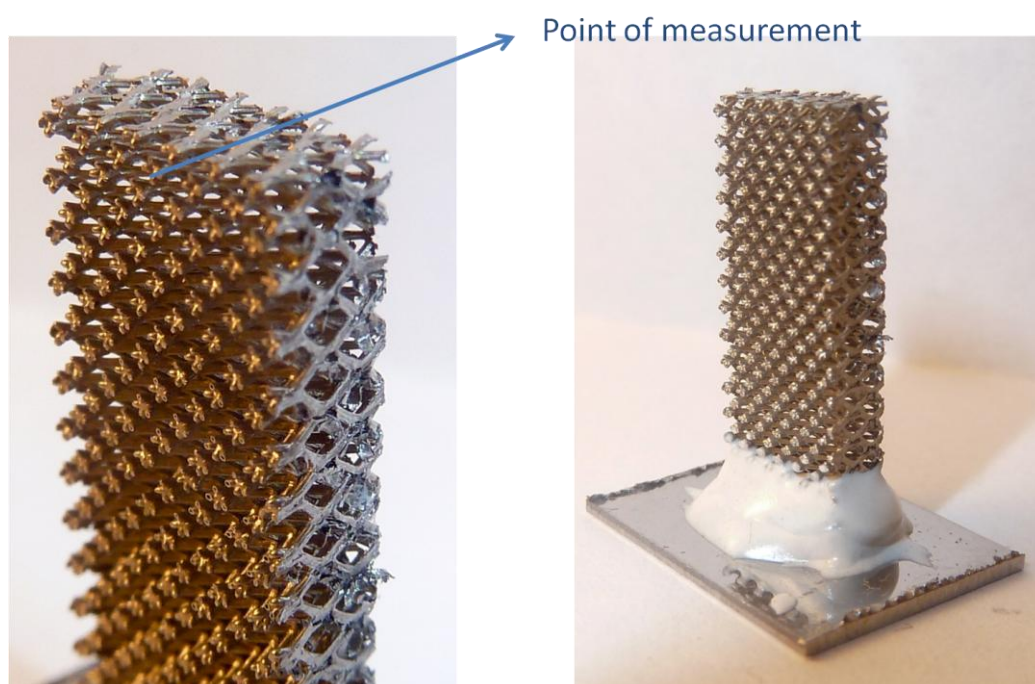


Figure 14: Plate without polymer



2.7. Procedure

Once we got the four samples we were ready to use the MSA-500 Micro System Analyzer.

Here we can see the procedure followed:

- Sweep of frequencies until 20 kHz finding the first mode of resonance of each sample
- Stepped sine test around the peak of resonance with steps of 0.1Hz
- Data obtained: Velocity of displacement ($\mu\text{m/s}$) versus Frequency (Hz)
- Measured: At the extreme point of each sample, see Figures 11 to 14

2.8. Results

For each type of truss (with and without polymer) we obtained data of velocity vs. frequency. In the following graphics, see Figures 15 and 16 we can see each peak corresponding to each first vibrational mode.

Once we got all the information about the vibration behavior of the samples, we were able to calculate the dynamic parameters in order to compare the results using or not polymer inside the structure.



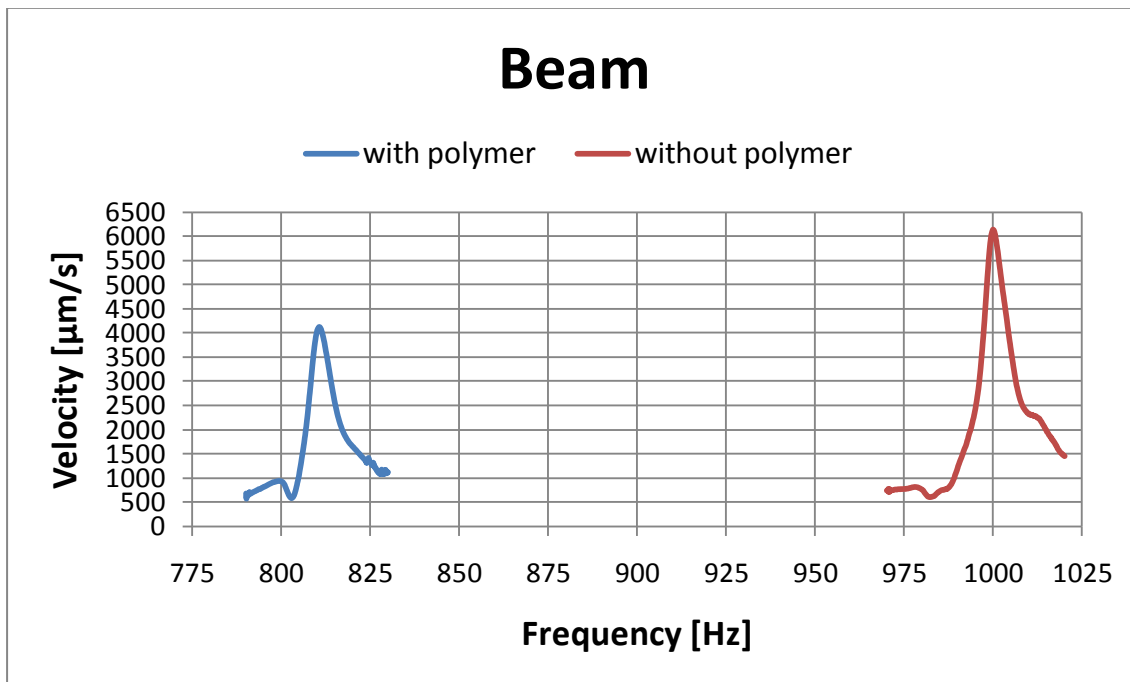


Figure 15: First vibrational mode for beam samples

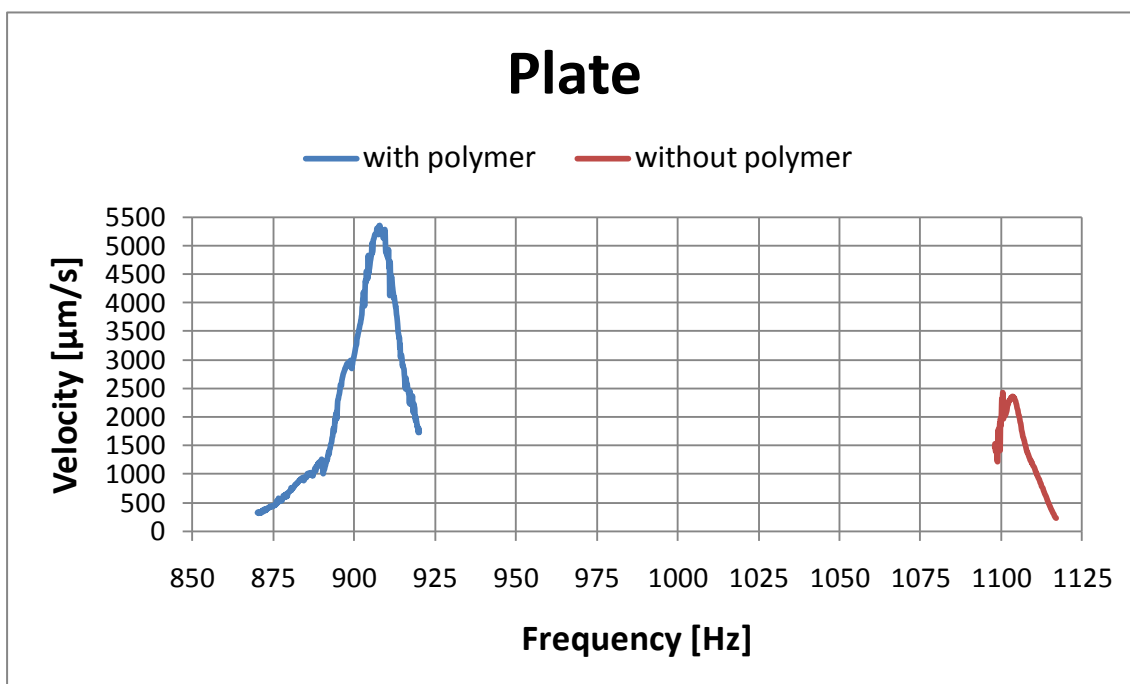


Figure 16: First vibrational mode for plate samples



2.9. Processing the results

Our objective on the first part of this project was to get the dynamic parameters for each sample. In order to do that we performed a curve fitting on the experimental data obtained during the test. The curve fitting was carried out around each of the peaks you see in Figures 15 and 16 (first vibrational mode).

We calculated the dynamic parameters using the classic viscoelastic system, and assuming that our sample had the same response.

2.9.1. Viscoelastic system

We used the general viscoelastic system to obtain an equation with the dynamic parameters of a viscoelastic system but as a function of the previous data (velocity and frequency)

In the Figure 17 we can see a sketch of a viscoelastic system:

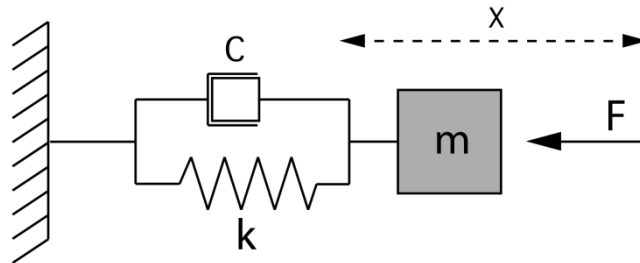


Figure 17: Viscoelastic sytem

If we study all the forces applied on the previous system, we can express the differential system in terms of the displacement x .

$$F = m\ddot{x} + c\dot{x} + kx$$

If we apply the Laplace transform,

$$F(s) = (s^2m + sc + k)X(s)$$



$$\frac{X(s)}{F(s)} = \frac{1}{s^2m + sc + k}$$

We want to find an expression of the velocity because is the only data obtained during the test. So we derive the previous equation.

$$\frac{\dot{X}(s)}{F(s)} = \frac{As}{s^2m + sc + k}$$

We have interest in the frequency response, so we replace $s = jw$

$$\frac{\dot{X}(s)}{F(s)} = \frac{Ajw}{(jw)^2m + jwc + k}$$

Finally we calculate the modulus of the previous equation to have a relation between velocity and frequency.

$$\left| \frac{\dot{X}(s)}{F(s)} \right| = \frac{Aw}{\sqrt{(cw)^2 + (k - mw^2)^2}}$$

2.9.2. Curve fitting

After the previous calculation of the relation between velocity and frequency in a viscoelastic system, now using *Matlab*® [7] we fitted a curve by least-squares method in order to get all the dynamic parameters defined in a viscoelastic system (c,k,m).

$$\left| \frac{\dot{X}(s)}{F(s)} \right| = \frac{Aw}{\sqrt{(cw)^2 + (k - mw^2)^2}}$$

Where,

$X(s)$: displacement

$F(s)$: applied force



A : parameter

c : damping coefficient (g/s)

k : spring constant (mN/m)

m : mass (g)

With the *Matlab*[®] tool we got the following graphs, see Figure 18 to 21 with the values of A , c , k and m .

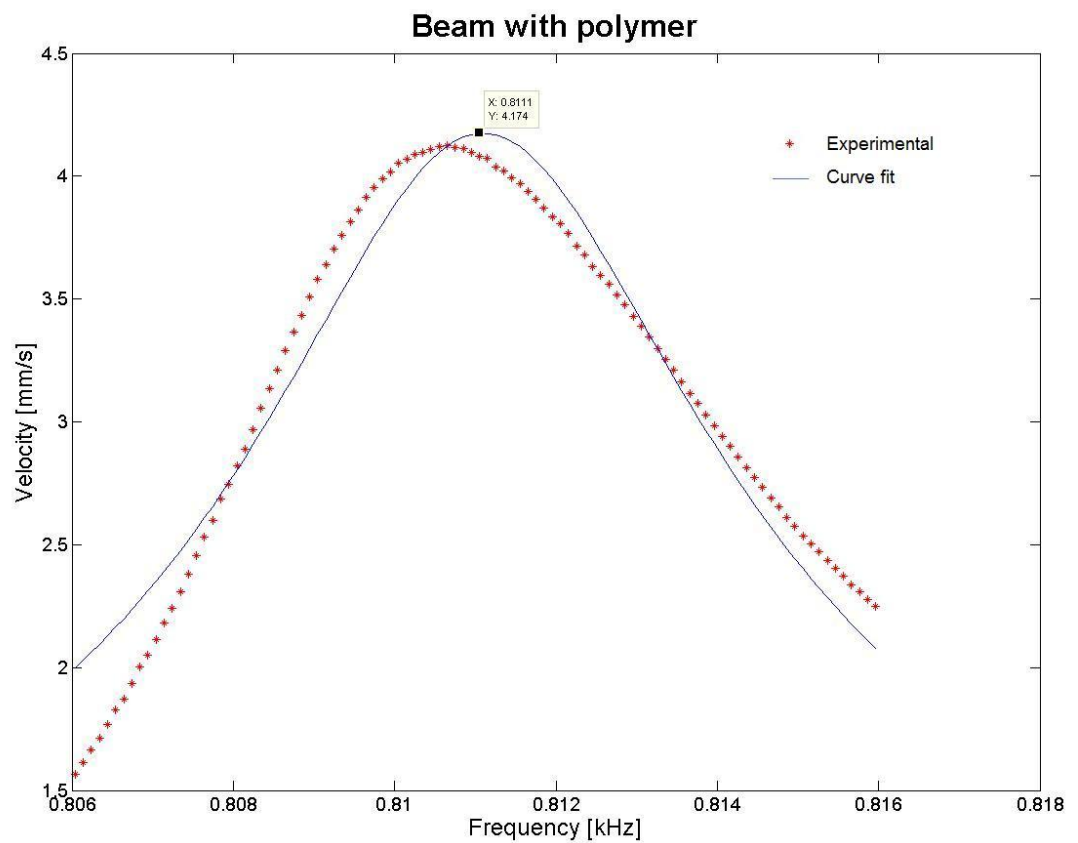


Figure 18: Curve fitting



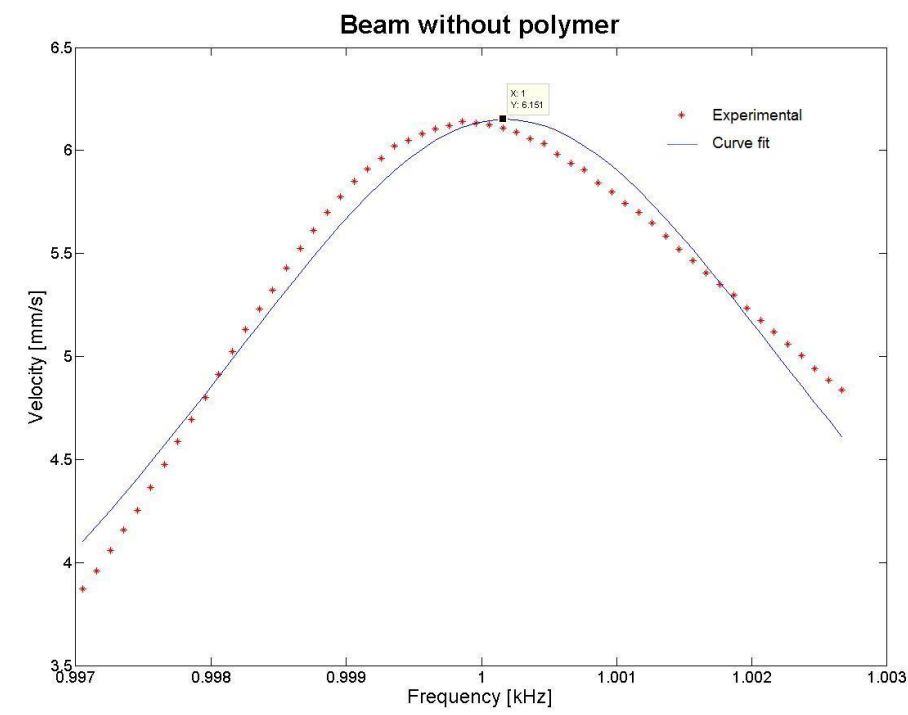


Figure 19: Curve fitting

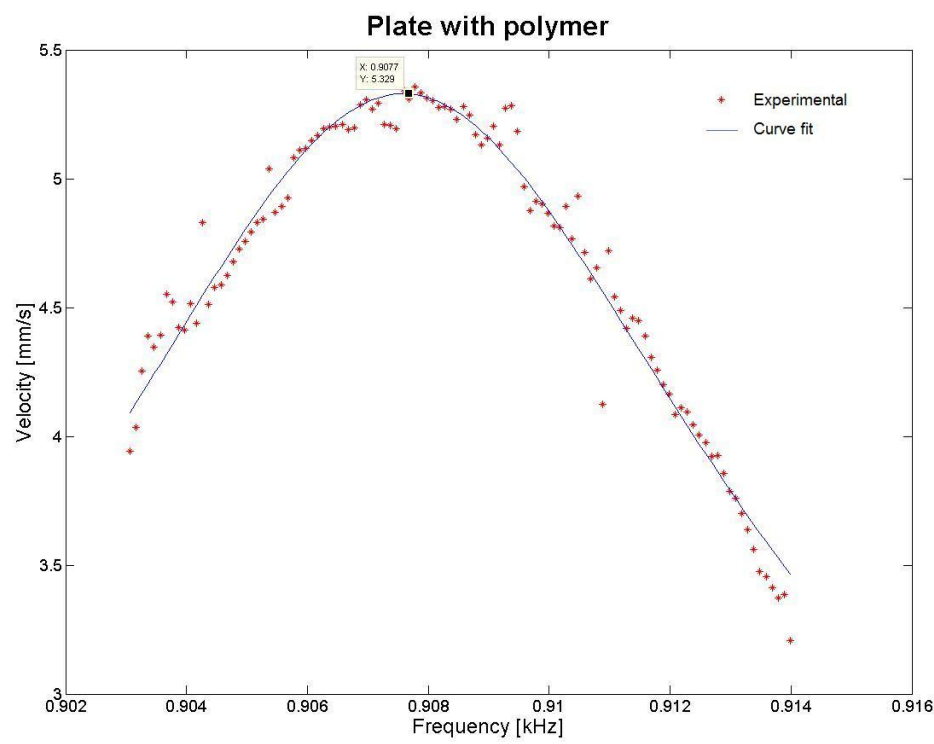


Figure 20: Curve fitting



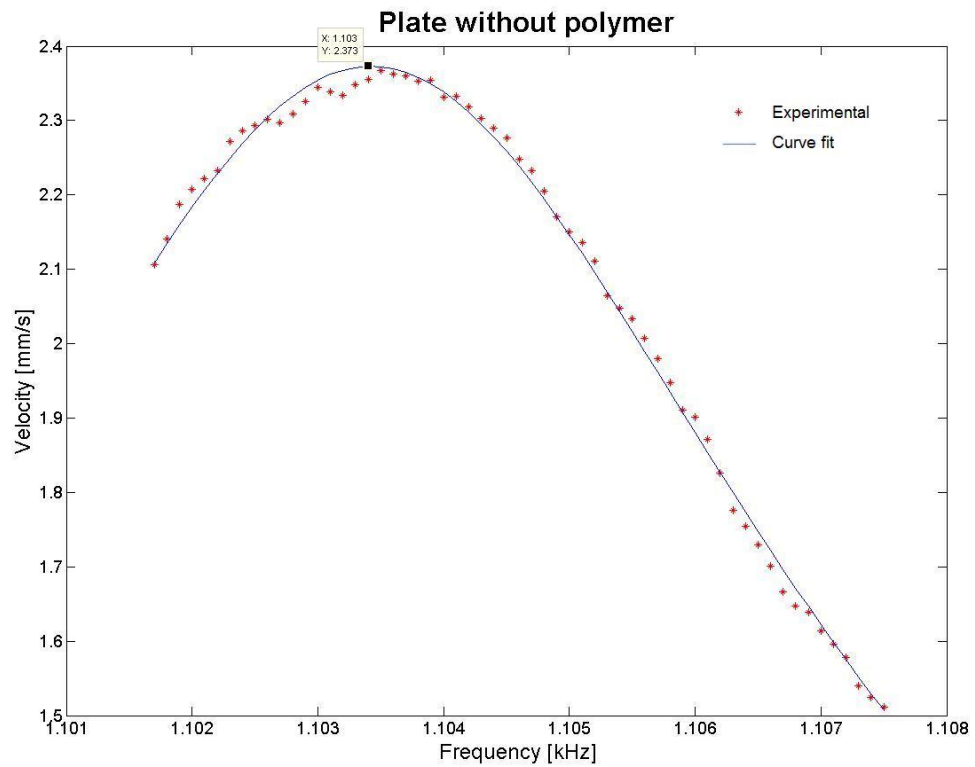


Figure 21: Curve fitting

2.10. Analysis of the results

Once we got the curve fitting graphs we could complete the following table with the results of the test. A , c , k , and m were obtained with the curve fitting, but $\tan \delta$ and Q factor were calculated using the following formulas:

$$\tan \delta = \frac{c}{\sqrt{km}} \quad Q^{-1} \approx \sqrt{3} \tan \delta$$



		Peak [Hz]	A	c [g/s]	k [mN/m]	m [g]	$\tan \delta$	Q
Beam	with polymer	811	0.0319	0.0077	1.8128	2.2350	0.00383	150.9254
Beam	without polymer	1000	0.0312	0.0051	1.8091	1.8088	0.00282	204.7839
Plate	with polymer	908	0.0556	0.0104	1.5796	1.7404	0.00627	92.04583
Plate	without polymer	1103	0.0112	0.0047	1.7142	1.5536	0.00288	200.4665

This results show us all the necessary information to see how the system's damping is. The numbers $\tan \delta$, c coefficient and Q factor explain the damping of the material[8]. A greater $\tan \delta$ and c coefficient means a higher damping of the system, and the same but with lower Q factor.

In the following table we can see a quick summary of the results:

	Polymer	NO Polymer
Q	↓	↑
$\tan \delta$	↑	↓
c	↑	↓



2.11. Conclusions

In this first part of this project we could show some interesting points. First, we concluded that the MSA-500 Micro System Analyzer is a good equipment to carry out measurements of vibrations in a micro/nano scale and allowed us to calculate the dynamic Parameters of the Micro-Architected Materials.

Then, as explained in section 2.2 *Manufacturing Technologies* the original idea of HRL Laboratories was to use polymer as a mold for manufacturing the metallic truss and then to remove this polymer to have just the metallic truss. But with this experiment we can conclude that the $\tan \delta$ and c coefficient are greater when we have polymer inside the truss. This means that the polymer helps to increase the damping effect in the material.

So it could be considered for the future to keep the polymer inside the micro-architected material as a new line of investigation. So in case a characteristic of low density truss is important, truss without polymer could be the approach but if it is better to have a higher damping of the truss regardless of his density then a truss with polymer could be the approach.

Proposal for future investigation is to characterize the truss for both types, without polymer and with polymer inside, by carrying out enough trials in the MSA-500 Micro System Analyzer.



3. Tunable combinations of stiffness and damping by employing negative stiffness elements

3.1. General overview

Continuing with the idea to obtain materials with better properties our goal in this second part of the project was to show the possibility to make materials with higher combination of stiffness and damping, improving the current ones.

The starting point of this new investigation line was based on the papers of Roderic Lakes, professor at University of Wisconsin, an expert in viscoelastic materials. Professor Lakes published many papers about negative stiffness concept[1] and how this can help to create systems with higher properties.

In this part of the project we showed, in a theoretical/mathematical way, how to use negative stiffness elements to increase the properties of materials, and we proposed a new negative stiffness element with interesting properties to create this material in a future work.

3.2. Negative stiffness concept

In mechanics, stiffness refers to the ratio of the generalized force to the generalized displacement. For a spring the stiffness is the ratio of the force to the displacement: the usual spring constant k . For a three-dimensional solid viewed as a continuum in the context of elasticity theory, the measure of stiffness is the ratio of the stress (force per area) to the strain (displacement per length), referred to as a modulus. This definition is true when we are talking about positive stiffness. So what is negative stiffness?

Physically, when an elastic object is pressed, we expect it to resist by exerting a restoring force. This is called positive stiffness, which occurs when the deformation is



in the same direction as the applied force, corresponding to a restoring force that returns the deformable body to its neutral position. A reversal of this restoring force corresponds to negative stiffness. In this case when we apply a load the displacement is increased and deformable body doesn't return to its neutral position. This involves that negative stiffness elements is always an unstable element for itself.

In the Figure 22 we show an example of the difference between negative and positive stiffness elements.

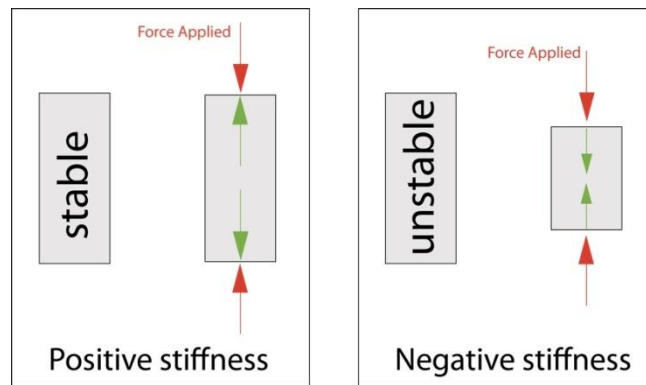


Figure 22: Positive stiffness vs negative stiffness

Although any element with negative stiffness is unstable for itself, if this element is combined in the proper way with other positive stiffness elements then better properties can be achieved.

In this part of this project we tried to use the idea of using materials with negative stiffness to increase the damping coefficient or the stiffness of a mechanic system. In order to do that, we were thinking about which negative stiffness element we should use for our system.



3.3. Example of negative stiffness system

Professor Roderic Lakes has been working on this idea during many years. In his papers he normally used mechanical elements with negative stiffness. Here you can see one of these mechanisms as an example.

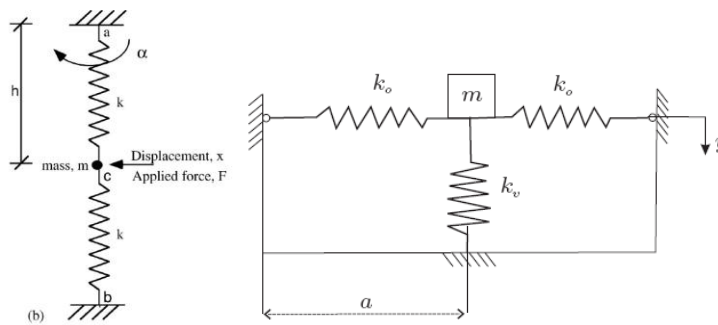


Figure 23: Examples of negative stiffness systems

These systems have both a mass in an unstable point. If a small force is applied this mass is automatically moved out of this point. This mass is an unstable point due to springs are not in their neutral position, they are compressed. Once we displace the mass from the unstable point of equilibrium, springs never get back to the initial position. Both systems are examples of negative stiffness, but they use mechanic elements.

3.4. Capacitor: Tunable negative stiffness element

There are many elements or mechanisms with negative stiffness, but we looked for a controllable element having the opportunity to modify the mechanical properties of the system.

We thought to use a capacitor as an element with negative stiffness. As it is known a parallel plate capacitor is an unstable system. If we have different voltage on each plate the attraction of these plates increases depending of the distance. When a load is applied the distance is reduced and the attraction is increased, so that means we



have a negative stiffness element. We can better understand it using the negative stiffness formula[9] for a parallel plate capacitor.

$$K = -\frac{\varepsilon_0 S}{g^3} V_{dc}^2$$

Where,

ε_0 is the dielectric constant of vacuum

S is the cross-sectional area

g is the plate capacitor gap

V_{dc} is voltage applied

The most interesting part of using a parallel plate capacitor as a negative stiffness element is that its negative stiffness can be tunable modifying the voltage applied. This idea let us to think about the possibility to make a material with tunable properties just adjusting the voltage. In addition, in the papers of Roderic Lakes[1] we can read that the most difficult part when we use negative stiffness elements is to stabilize the system, combining elements of positive stiffness and negative stiffness. This is because there is a relation between the positive stiffness and negative stiffness to be in the stability region. So we thought that using a parallel plate capacitor with a tunable negative stiffness could allow us to stabilize the system, and at the same time modify the material properties being always in the stability region.

3.5. Mechanical model

After we decided to use a capacitor as a negative stiffness element, we had to decide the mechanical model and its stability conditions.

We used the Roderic Lakes' paper[1] Stable extremely-high-damping discrete viscoelastic systems due to negative stiffness elements. In his paper Lakes proposed the following mechanical model as a system with high damping due to negative stiffness elements.



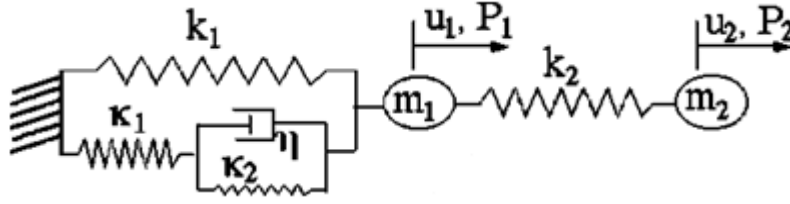


Figure 24: Lakes' model[1]

First we decided to simplify the mechanical model using only 3 “springs”, 2 of them with positive stiffness (k_1 and k_2) and the other one with negative stiffness $k_1 < 0$. Before continuing let us clarify that we use another nomenclature in this project. For sake of clarity we will note k_1 as k , k_1 as t_1 and k_2 as t_2 . The negative stiffness element is t_1 .

In the Figure 25 we can see the first simplification of the Lakes' model:

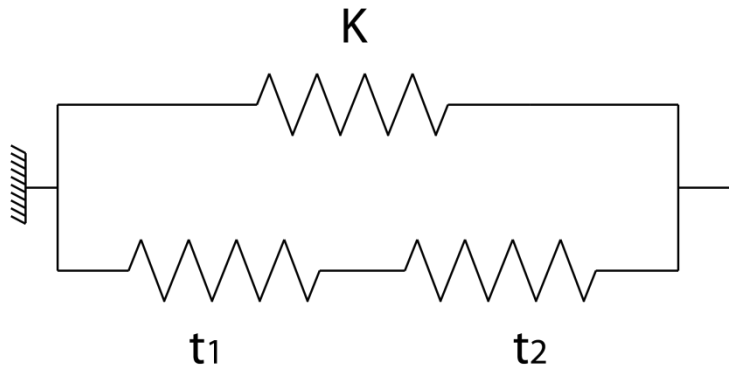


Figure 25: First simplification of Lakes' model

In this system k and t_2 are springs with positive stiffness and t_1 is a capacitor(negative stiffness element).

With this simplification we will focus our study in the displacement of the right node when a load is applied.

Our first objective was to calculate the k_{eq} of the system (global stiffness). With k_{eq} value we are able to predict the stiffness of the global system and its stability. We compute k_{eq} in order to guess the magnitude we can achieve if a negatives stiffness element is allowed in our mechanism.



Our goal is to show $k_{eq} \gg k$ in a stable system, of course.

To calculate k_{eq} , first we compute $t_{1,2}$ in serial configuration and then we add k in parallel configuration.

$$\frac{1}{t_{1,2}} = \frac{1}{t_1} + \frac{1}{t_2} \Rightarrow t_{1,2} = \frac{t_1 t_2}{t_1 + t_2}$$

$$k_{eq} = t_{1,2} + k \Rightarrow k_{eq} = \frac{t_1 t_2}{t_1 + t_2} + k$$

Which give the equivalent stiffness of the system:

$$k_{eq} = \frac{t_1 t_2}{t_1 + t_2} + k$$

To analyze this equation, the initial idea is to maximize the stiffness including a negative stiffness element.

So at this point we had an equation to maximize with some conditions:

$$k_{eq} = \frac{t_1 t_2}{t_1 + t_2} + k$$

$$k_{eq}, k, t_2 > 0; t_1 < 0$$

The next step was to analyze the system from a mathematical point of view.

Once we did a previous study of the simplified system we decided to modify the initial mechanic system and we carried out a deepest mathematical study of the system stability due to using negative stiffness elements the most important part to study is the stability one.

We introduced a damper in the system because professor Lakes used it in his models and we wanted to understand if it was crucial for the system stability.



3.6. Differential system formulation

In the following illustration we have a sketch of the viscoelastic system studied:

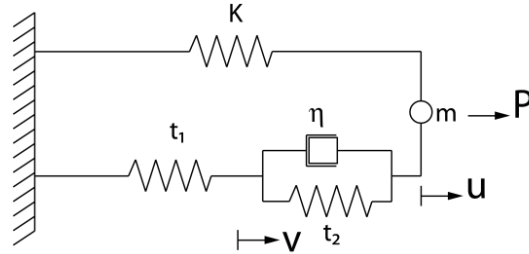


Figure 26: Viscoelastic system

Let's call the *upper branch* where the spring k is. We call the *lower branch* the next one.

The external load applied on the system is P , the positive displacement to the right side u and w the derivative of u ($w = u'$), being f the strength of the *lower branch*.

An auxiliary variable v is used as the displacement of the t_1 constant spring (positive to the right side)

Then we could evaluate these equations:

$$u' = w; \quad mu'' = -ku - f + P \quad \Leftrightarrow \quad w' = -\frac{k}{m}u - \frac{1}{m}f + \frac{P}{m}$$

Calculating f force as a function of the *lower branch* system elements:

$$f = vt_1 = (u - v)t_2 + (u' - v')\eta$$

With these equalities we want to get a f' expression in function of f , u and w so it wasn't necessary to use the auxiliary variable v anymore.

As $f = vt_1$ we have $v = f/t_1$ and the derivative is $v' = f'/t_1$, we can obtain:



$$f = (u - v)t_2 + (u' - v')\eta \Leftrightarrow f = ut_2 - \frac{f}{t_1}t_2 + w\eta - \frac{f'}{t_1}\eta$$

Finding f' we get:

$$f' = \frac{t_1 t_2}{\eta} u + t_1 w - \frac{t_1 + t_2}{\eta} f$$

Therefore, we had to study the solutions (and their stability) of the following differential system:

$$\begin{pmatrix} u' \\ w' \\ f' \end{pmatrix} = \begin{pmatrix} 0 & 1 & 0 \\ -\frac{k}{m} & 0 & -\frac{1}{m} \\ \frac{t_1 t_2}{\eta} & t_1 & -\frac{t_1 + t_2}{\eta} \end{pmatrix} \begin{pmatrix} u \\ w \\ f \end{pmatrix} + \begin{pmatrix} 0 \\ \frac{P}{m} \\ 0 \end{pmatrix} = A \cdot \begin{pmatrix} u \\ w \\ f \end{pmatrix} + \begin{pmatrix} 0 \\ \frac{P}{m} \\ 0 \end{pmatrix}$$

If (u_e, w_e, f_e) is a stable point then $(u'_e, w'_e, f'_e) = (0, 0, 0)$ so,

$$\begin{pmatrix} u_e \\ w_e \\ f_e \end{pmatrix} = -A^{-1} \cdot \begin{pmatrix} 0 \\ \frac{P}{m} \\ 0 \end{pmatrix}$$

The matrix A determinant is

$$|A| = -\frac{t_1 t_2 + k(t_1 + t_2)}{m\eta}$$

And the inverse matrix is:

$$A^{-1} = \frac{1}{|A|} \begin{pmatrix} \frac{t_1}{m} & \frac{t_1 + t_2}{\eta} & -\frac{1}{m} \\ -\frac{t_1 t_2}{m\eta} - \frac{k(t_1 + t_2)}{m\eta} & 0 & 0 \\ -\frac{kt_1}{m} & \frac{t_1 t_2}{\eta} & \frac{k}{m} \end{pmatrix}$$



The result is:

$$(u_e, w_e, f_e) = \left(\frac{P(t_1 + t_2)}{t_1 t_2 + k(t_1 + t_2)}, 0, \frac{P t_1 t_2}{t_1 t_2 + k(t_1 + t_2)} \right)$$

Our interest is in the first component, which is the equilibrium displacement of the system.

$$u_e = \frac{P(t_1 + t_2)}{t_1 t_2 + k(t_1 + t_2)}$$

Our final goal is to study the stiffness and damping of this system. In order to do this in the easiest way we only have to calculate the displacement in the equilibrium position when we apply a unit force P . Then the stiffness will be the inverse of the equilibrium position u_e .

3.6.1. Stability study

Stability study is the main section of this part. Including a negative stiffness element the stability of the system is a critic point. In this part of the project we will try to find a stability region of values where the system is stable and the properties can be increased.

The stability of the system is equivalent to the fact that all three eigenvalues of the matrix A has a negative real part. Hurwitz criterion[10] establishes equivalent conditions depending only on the elements of A .

The characteristic polynomial of A is:

$$\begin{aligned} |A - xI| &= \begin{vmatrix} -x & 1 & 0 \\ -k & -x & -1 \\ \frac{m}{t_1 t_2} & t_1 & -\frac{t_1 + t_2}{\eta} - x \end{vmatrix} \\ &= -x^3 - \frac{t_1 + t_2}{\eta} x^2 - \frac{k + t_1}{m} x - \left(\frac{k(t_1 + t_2) + t_1 t_2}{m\eta} \right) \end{aligned}$$



We need to change the coefficient signs in order to make the leading coefficient $a_0 > 0$ and the polynomial becomes:

$$x^3 + \frac{t_1 + t_2}{\eta}x^2 + \frac{k + t_1}{m}x + \left(\frac{k(t_1 + t_2) + t_1 t_2}{m\eta}\right)$$

According to Hurwitz criterion, if $P(x) = a_0x^3 + a_1x^2 + a_2x + a_3$ is a polynomial with $a_0 > 0$ we must create the following matrix:

$$H = \begin{pmatrix} a_1 & a_3 & 0 \\ a_0 & a_2 & 0 \\ 0 & a_1 & a_3 \end{pmatrix}$$

and then calculate the central determinants

$$\Delta_1 = a_1, \quad \Delta_2 = a_1a_2 - a_0a_3, \quad \Delta_3 = a_3\Delta_2$$

A necessary and sufficient condition for $P(x)$ to have the three roots with negative real part is:

$$\Delta_1 > 0, \quad \Delta_2 > 0, \quad \Delta_3 > 0.$$

In our case:

$$a_0 = 1; \quad a_1 = \frac{t_1 + t_2}{\eta}; \quad a_2 = \frac{k + t_1}{m}; \quad a_3 = \frac{k(t_1 + t_2) + t_1 t_2}{m\eta}$$

And the central determinants are:

$$\Delta_1 = \frac{t_1 + t_2}{\eta} > 0, \quad \Delta_2 = \frac{t_1^2}{m\eta} > 0, \quad \Delta_3 = \Delta_2 \frac{k(t_1 + t_2) + t_1 t_2}{m\eta} > 0$$

As m and η are positive, previous conditions can be written as:

$$t_1 + t_2 > 0; \quad t_1^2 > 0; \quad k(t_1 + t_2) > -t_1 t_2$$

Knowing that $t_1 < 0$ we could rewrite the first condition as $t_2 > |t_1|$ and the second condition is always true.



In the one hand, $t_1 + t_2 > 0$ is the upper-right half plane defined by the line $t_1 + t_2 = 0$, but as $t_1 < 0$ the area of study is bounded by the axis $t_2 > 0$ and the line $t_1 + t_2 = 0$.

In the other hand $k(t_1 + t_2) > -t_1 t_2$ is the region defined by the rectangular hyperbola $k(t_1 + t_2) = -t_1 t_2$ which contains the first quadrant.

With these conditions we plot the previous defined region in the plane of coordinates t_1 and t_2 (dark gray). This is the stability system region.

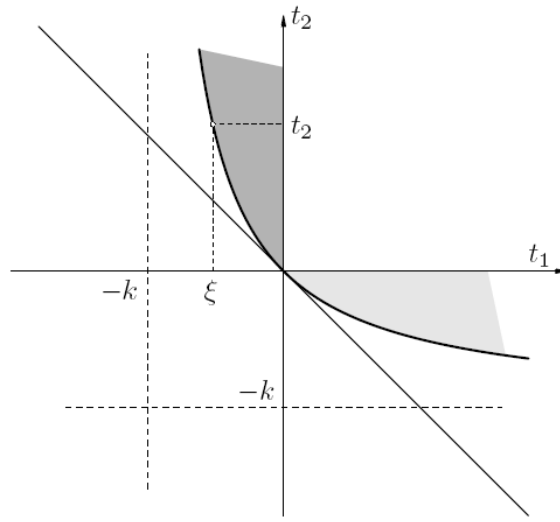


Figure 27: Stability system region

Since $u_e = \frac{(t_1+t_2)}{t_1 t_2 + k(t_1+t_2)}$ we have $\frac{1}{u_e} = k_{eq} = k + \frac{t_1 t_2}{t_1+t_2}$ and at $t_1 t_2 < 0$ s, $t_1 + t_2 > 0$ we have $k_{eq} = k + (\text{something negative}) < k$. But $t_1 t_2 + k(t_1 + t_2) > 0$ implies $\frac{t_1 t_2}{t_1+t_2} > -k$ and $k_{eq} > 0$. Both conditions can be written $k_{eq} \in (0, k)$.

If we choose a value for k and for t_2 , the stability range for t_1 is between ξ and 0 (negative values). If t_1 was positive, then t_2 should be negative and the stability range would be between ξ and 0 as well. That case is painted with light gray. The first quadrant is the stability area in case that $t_1 > 0$ and $t_2 > 0$.



To calculate the ξ value we have to use the rectangular hyperbola equation.

$$k(t_1 + t_2) = -t_1 t_2 \quad \Rightarrow \quad k(t_1 + t_2) + t_1 t_2 = 0$$

In the stability boundary $\xi = t_1$ then,

$$\xi = -\frac{kt_2}{k + t_2}$$

So once we fix the k and t_2 values, $|\xi|$ is the maximum value that t_1 can achieve to make the system stable.

3.7. Alternative formulation of the differential system

The previous differential system involved the variables u, w, f as in Lakes' approach. Now we present here a more classical (and equivalent) method, dealing with u, v space and velocity variables.

We do that to have another way to focus and discuss the problem and to be sure that everything is consistent.

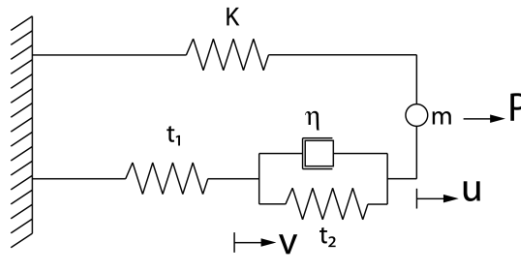


Figure 28: Viscoelastic system

So we have the following relations:

$$u' = w \quad (1) \quad mu'' = -ku - f + P \quad (2)$$



Then we get f in order to find the relation between the displacements.

$$f = t_1 v = t_2(u - v) + \eta(u' - v')$$

$$\eta v' = t_2 u - (t_1 + t_2)v + \eta u'$$

$$\eta v' = t_2 u - (t_1 + t_2)v + \eta w \quad (3)$$

$$\text{With } f = t_1 v, (1) \text{ and } (2) \text{ result in } mw' = -ku - t_1 v + P \quad (4)$$

With (1), (3) and (4) the system is,

$$\begin{pmatrix} u' \\ v' \\ w' \end{pmatrix} = \begin{pmatrix} 0 & 0 & 1 \\ \frac{t_2}{\eta} & -\frac{t_1 + t_2}{\eta} & 1 \\ -\frac{k}{m} & -\frac{t_1}{m} & 0 \end{pmatrix} \begin{pmatrix} u \\ v \\ w \end{pmatrix} + \begin{pmatrix} 0 \\ 0 \\ \frac{P}{m} \end{pmatrix}$$

If (u_e, w_e, f_e) is a stable point then $(u'_e, w'_e, f'_e) = (0, 0, 0)$ so,

$$\begin{pmatrix} u_e \\ v_e \\ w_e \end{pmatrix} = - \begin{pmatrix} 0 & 0 & 1 \\ \frac{t_2}{\eta} & -\frac{t_1 + t_2}{\eta} & 1 \\ -\frac{k}{m} & -\frac{t_1}{m} & 0 \end{pmatrix}^{-1} \begin{pmatrix} 0 \\ 0 \\ \frac{P}{m} \end{pmatrix}$$

Therefore, if $|A| = -\frac{t_1 t_2 + k(t_1 + t_2)}{m\eta}$ is the determinant of A ,

$$\begin{pmatrix} u_e \\ v_e \\ w_e \end{pmatrix} = -|A|^{-1} \begin{pmatrix} \frac{t_1}{m} & -\frac{t_1}{m} & \frac{t_1 + t_2}{\eta} \\ \frac{k}{m} & \frac{k}{m} & \frac{t_2}{\eta} \\ -t_1 t_2 - \frac{k(t_1 + t_2)}{m\eta} & 0 & 0 \end{pmatrix} \begin{pmatrix} 0 \\ 0 \\ \frac{P}{m} \end{pmatrix} = \begin{pmatrix} \frac{P(t_1 + t_2)}{t_1 t_2 + k(t_1 + t_2)} \\ \frac{P t_2}{t_1 t_2 + k(t_1 + t_2)} \\ 0 \end{pmatrix}$$



3.7.1. Stability study

We wanted to be sure that the stability of this system is the same with this alternative formulation. The characteristic polynomial of the matrix A is:

$$\begin{vmatrix} -x & 0 & 1 \\ \frac{t_2}{\eta} & -\frac{t_1+t_2}{\eta} - x & 1 \\ -\frac{k}{m} & -\frac{t_1}{m} & -x \end{vmatrix} = -x^3 - \frac{t_1+t_2}{\eta}x^2 - \frac{k+t_1}{m}x - \left(\frac{k(t_1+t_2) + t_1t_2}{m\eta}\right)$$

We could observe that the result is the same polynomial studied before, then we could say that we have the same stability conditions.

3.8. Real parts of the eigenvalues

In this section we want to see the results of the system stability in terms of the real part of each eigenvalue. In order to do that we did a numerical computation and then we could plot the graphic result.

We use these values to plot the followings graphs in all the next sections of this project as in Lakes' paper.

$$k = 10 \text{ kN/m}; \quad m = 10^{-12} \text{ kg}; \quad t_2 = 5 \text{ kN/m}; \quad \eta = 0.01, 0.1, 0.3; \quad t_1 \in [-5, 0] \text{ kN/m}$$

The characteristic polynomial has one real root and two complex conjugate roots, this is the reason why we only see two curves, because the real parts for the two complex conjugate roots are equal. One of them is always below X-axis so it is always negative. The other one cross the axis in the point ξ (limit of stability).

We previously calculated the ξ value respect k and t_2 values, so in order to see that everything is consistent the ξ value is:

$$\xi = -\frac{kt_2}{k+t_2} = -\frac{10 \cdot 5}{10+5} = -\frac{50}{15} = -3.33$$



The derivative values at the point ξ (where graphic cross X-axis) are dependent on η coefficient. We sketch three graphs with different η values. Observe the increasing of tangent's slope at point $(\xi, 0)$ as η vanishes.

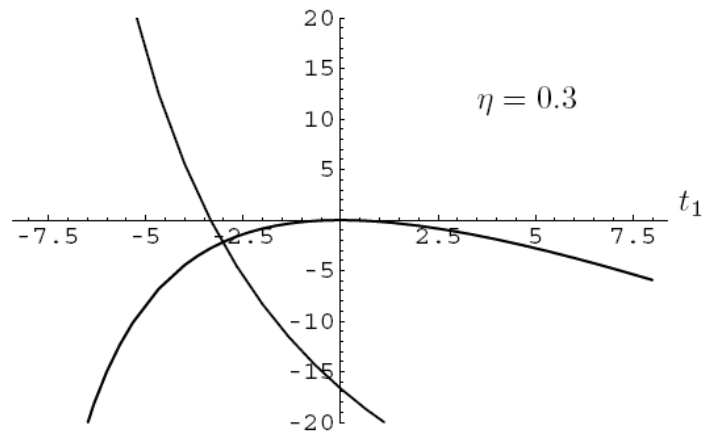


Figure 29: Graph of the real part of the eigenvalues when $\eta=0.3$

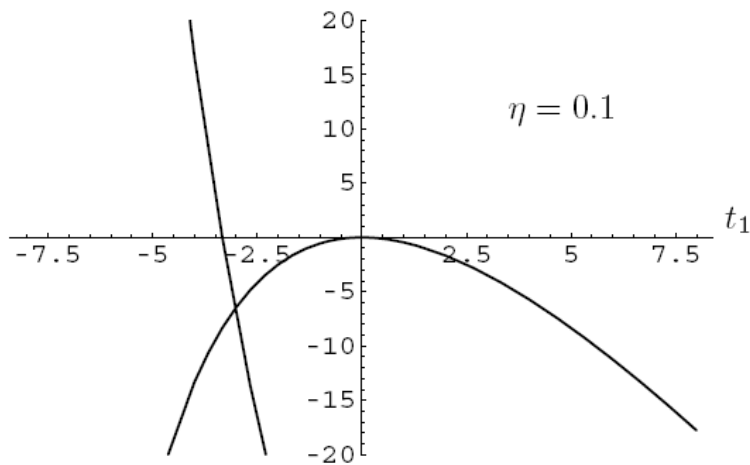


Figure 30: Graph of the real part of the eigenvalues when $\eta=0.1$



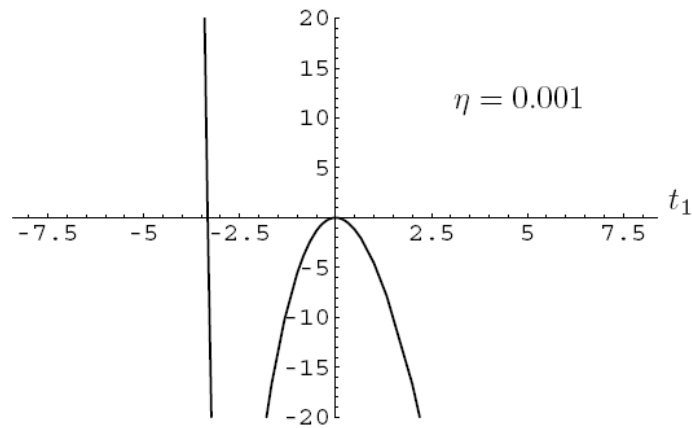


Figure 31: Graph of the real part of the eigenvalues when $\eta=0.001$

3.9. Imaginary parts of the eigenvalues

The imaginary parts of the eigenvalues of the system are almost constant. This means that the resonance frequency of the system is almost independent of t_1 value. We used the same parameters and the frequency was around 500kHz.

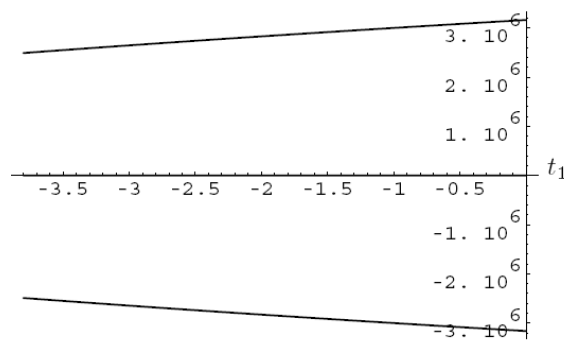


Figure 32: Graph of the imaginary part of the eigenvalues



3.10. Stability study using the central determinants graphs with Hurwitz criterion

The ξ value can be found using the central determinants that we calculated before when we used the Hurwitz criterion (see section 3.6.1.). If we plot graphics of the central determinants values in front of the t_1 value we can see that the first two values are always positive and the third is positive to the right of the ξ point. That means that we find the stability condition in the third graphic where the central determinant changes its sign.

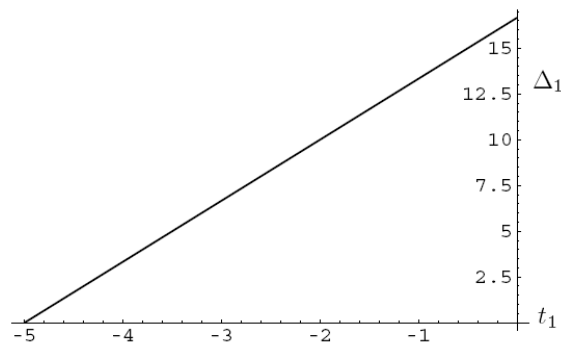


Figure 33: First central determinant in Hurwitz criterion

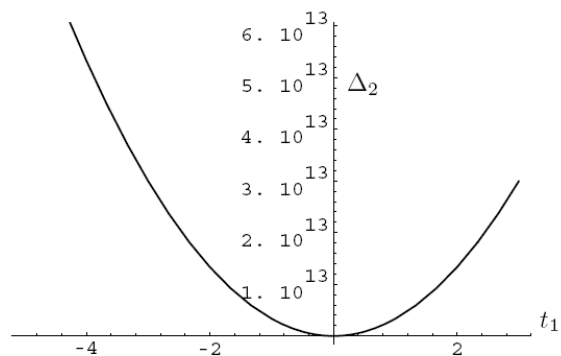


Figure 34: Second central determinant in Hurwitz criterion



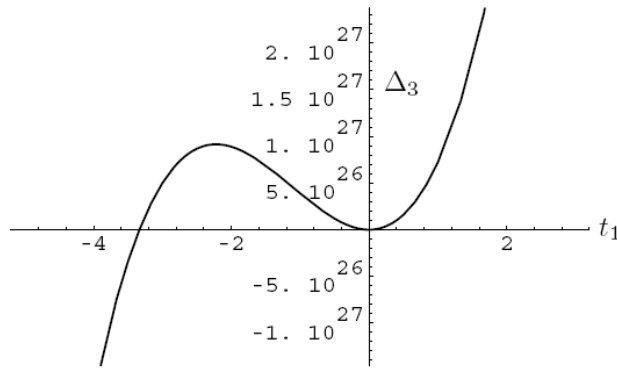


Figure 35: Third central determinant in Hurwitz criterion

3.11. Graphs of the system compliance (1/keff)

In order to see how is affected the stability by the negative stiffness element, we need to compute the compliance of the system on the stability region.

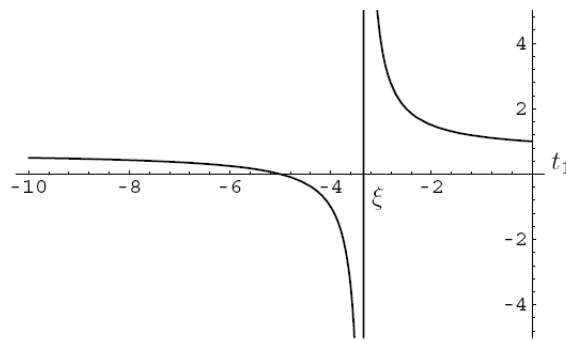
First of all, let us comment that compliance is a physic term that it is equivalent to the inverse of the stiffness, so it means that if we increase the compliance of the system, we are raising up the system's damping, but we are decreasing the system's stiffness.

In this project we can say that compliance is equal to u_e due to we assumed that the force P applied on the system was 1. Therefore, compliance is equivalent to,

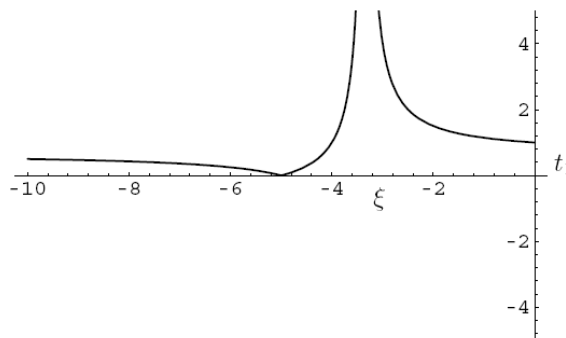
$$u_e = \frac{(t_1 + t_2)}{t_1 t_2 + k(t_1 + t_2)}$$

The following graph we plotted u_e against t_1 . The stability area is to the right of ξ value, where the vertical asymptote is.



Figure 36: Graph of u_e against t_1

We plotted a similar graph but doing the absolute value of the compliance $|u_e|$. The stability area is still to the right of the ξ value.

Figure 37: Graph of $|u_e|$ against t_1

As it can be shown in the graphics we can increase the compliance in the stability area. But in order to study this in a deepest way we will see in the next section the $\tan \delta$ coefficient [11] of the system using the Laplace transform.

3.12. Study of the system using Laplace transform

In order to get the stationary behavior of the system, supposing that it is stable, is more practical to use Laplace transform, because of it is not necessary to use the variation of the constants method or calculate the eigenvalues of the system.



We define the initial system as:

$$X' = AX + B$$

Where,

$$X = \begin{pmatrix} u \\ w \\ f \end{pmatrix}; \quad B = \begin{pmatrix} 0 \\ \frac{P}{m} \\ 0 \end{pmatrix}; \quad A = \begin{pmatrix} 0 & 1 & 0 \\ -\frac{k}{m} & 0 & -\frac{1}{m} \\ \frac{t_1 t_2}{\eta} & t_1 & -\frac{t_1 + t_2}{\eta} \end{pmatrix}$$

We can apply Laplace transform to the system denoting the transform with s subscript.

$$X_s - X_0 = AX_s + B_s$$

And taking zero as initial conditions,

$$(sI - A)X_s = B_s \quad \Rightarrow \quad X_s = (sI - A)^{-1}B_s$$

We can distinguish 3 cases for the vector B .

Case 1)

In this case we analyze the spontaneous behavior of the system, so this means we have an unforced system, where $B = \left(0, \frac{P}{m} \delta(0), 0\right)$ with δ the Dirac delta function. Therefore, B transform is $B_s = \left(0, \frac{P}{m}, 0\right)$. We can suppose afterwards $P = 1$ to simplify the computations, because P appears always as a factor.

We are interested in u_s the first component of X_s . So calculating,

$$u_s = \frac{N_s}{D_s} = \frac{\eta s + t_1 + t_2}{m\eta s^3 + m(t_1 + t_2)s^2 + \eta(k + t_1)s + k(t_1 + t_2) + t_1 t_2}$$



with

$$N_s = \eta s + t_1 + t_2$$

$$D_s = m\eta s^3 + m(t_1 + t_2)s^2 + \eta(k + t_1)s + k(t_1 + t_2) + t_1 t_2$$

And therefore, within the ranges of values of parameters which we move, and calculated numerically, this polynomial has one real root and two complex conjugate roots. These roots determine the system performance and stability.

Case 2)

In this second case we studied the behavior of the system when we apply a P constant force after an instant, for example, $t = 0$. So $H(0)$ is the Heaviside function with jump 1 at the origin, and $B = \left(0, \frac{P}{m}H(0), 0\right)$. Hence $B_s = \left(0, \frac{P}{m} \frac{1}{s}, 0\right)$ and doing $P = 1$ as we previously did,

$$u_s = \frac{\eta s + t_1 + t_2}{s(m\eta s^3 + m(t_1 + t_2)s^2 + \eta(k + t_1)s + k(t_1 + t_2) + t_1 t_2)} = \frac{N_s}{sD_s}$$

Using partial fractions decomposition,

$$u_s = \frac{N_s}{sD_s} = \frac{a}{s} + \frac{bs + c}{D_s} = \frac{aD_s + (bs + c)s}{sD_s}$$

Equating $s = 0$ then,

$$a = \frac{t_1 + t_2}{t_1 t_2 + k(t_1 + t_2)}$$

And the antitransform is,

$$u_e = \frac{t_1 + t_2}{t_1 t_2 + k(t_1 + t_2)}$$



Note that the terms belonging to

$$\frac{bs + c}{D_s}$$

are the oscillation terms of the free system itself, and if it is stable, vanish in the long run. These terms can only be calculated if we know the eigenvalues of the system, known only numerically.

Case 3)

Finally we studied the behavior of the system when we apply a sinusoidal force. In this case, $B = \left(0, \frac{P}{m} \sin \omega t, 0\right)$ and $B_s = \left(0, \frac{P}{m} \frac{\omega}{s^2 + \omega^2}, 0\right)$.

We find

$$\begin{aligned} u_s &= \frac{\omega(\eta s + t_1 + t_2)}{(s^2 + \omega^2)(m\eta s^3 + m(t_1 + t_2)s^2 + \eta(k + t_1)s + k(t_1 + t_2) + t_1 t_2)} \\ &= \frac{\omega N_s}{(s^2 + \omega^2)D_s} \end{aligned}$$

and using partial fractions decomposition,

$$u_s = \frac{\omega N_s}{(s^2 + \omega^2)D_s} = \frac{as + b}{s^2 + \omega^2} + \frac{cs + d}{D_s} = \frac{(as + b)D_s + (cs + d)(s^2 + \omega^2)}{(s^2 + \omega^2)D_s}$$

Equating $s = \omega i$ then,

$$a\omega i + b = \frac{\omega N_s(\omega i)}{D_s(\omega i)}$$

So,

$$a = \frac{-\eta \omega t_1^2}{((t_1 + t_2)(k - m\omega^2) + t_1 t_2)^2 + \eta^2 \omega^2 (k - m\omega^2 + t_1)^2}$$



$$b = \frac{\omega(t_1 + t_2)((t_1 + t_2)(k - m\omega^2) + t_1 t_2) + \eta^2 \omega^3 (k - m\omega^2 + t_1)}{((t_1 + t_2)(k - m\omega^2) + t_1 t_2)^2 + \eta^2 \omega^2 (k - m\omega^2 + t_1)^2}$$

and we can find the antitransform function,

$$a \cos \omega t + \frac{b}{\omega} \sin \omega t = M \sin(\omega t + \delta)$$

Using a and b values we can calculate M and $\tan \delta$

$$M^2 = a^2 + \frac{b^2}{\omega^2}; \quad \tan \delta = \frac{a\omega}{b}$$

The value of the complex modulus M depends strongly on the η value. The following graphs show M plotted against t_1 using $\eta = 0.3, 0.1, 0.01$

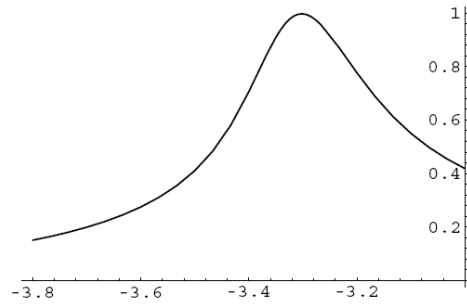


Figure 38: Graph of the complex modulus against t_1 when $\eta=0.3$

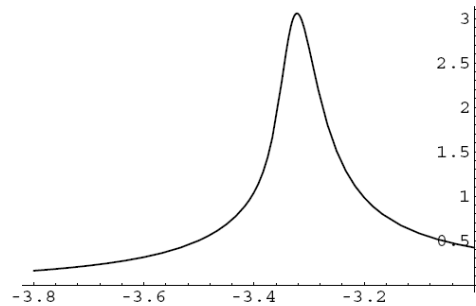


Figure 39: Graph of the complex modulus against t_1 when $\eta=0.1$



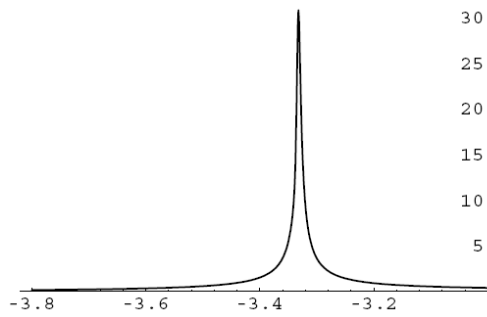


Figure 40: Graph of the complex modulus against t_1 when $\eta=0.01$

Otherwise, if we plot $|\tan \delta|$ with respect t_1 .

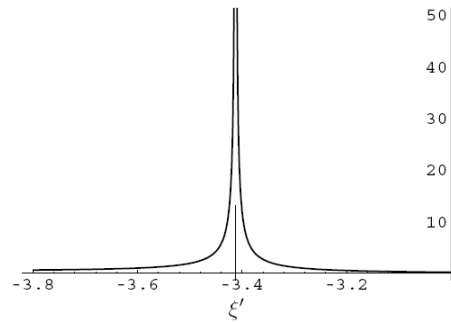


Figure 41: Graph of the $|\tan \delta|$ with respect t_1

and if we plot $|u_e \tan \delta|$ we get

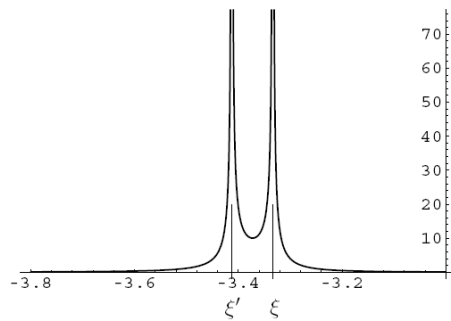


Figure 42: Graph of the $|u_e \tan \delta|$ with respect t_1



As we have seen before ξ value only depends on k and t_2 values, but ξ' value depends on η value. So, we deduce that $|\xi - \xi'|$ increases with η

But our real interest is to plot the product of stiffness and damping and see how the negative stiffness elements effects on it. The following graph corresponds to $\left| \frac{\tan \delta}{u_e} \right|$ against t_1 .

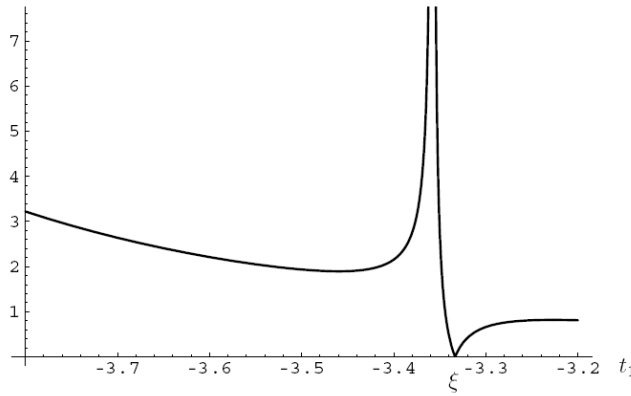


Figure 43: Graph of the $\left| \frac{\tan \delta}{u_e} \right|$ with respect t_1

We have a maximum in the stable region at the point $t_1 = -3.29593$ (negative stiffness) that corresponds to $\left| \frac{\tan \delta}{u_e} \right| = 0,349581 \text{ kN/m}$. If we compare with a $t_1 = 2$ (positive stiffness) value we have $\left| \frac{\tan \delta}{u_e} \right| = 0.00816 \text{ kN/m}$. This means an increase of 42,83 times.

In the following graphic we can see a zoom in the stability area. We have a maximum next to the stability limit where the properties of the system are increased.



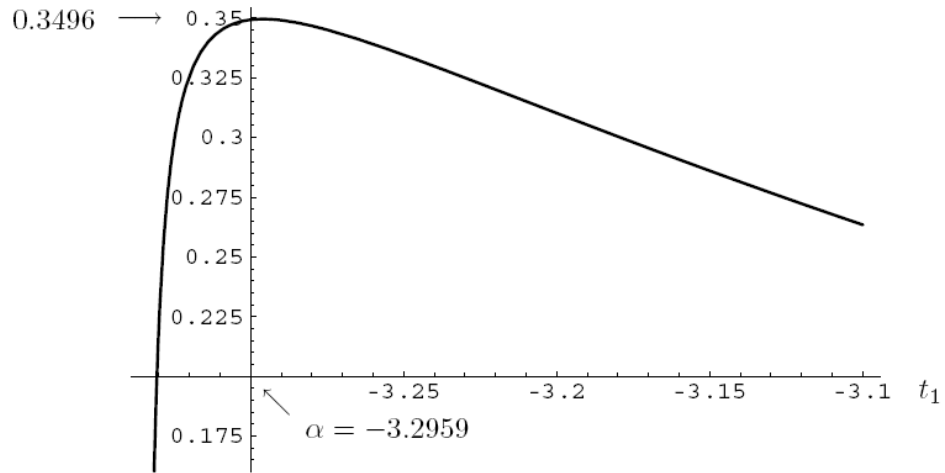


Figure 44: Graph of the $\left| \frac{\tan \delta}{u_e} \right|$ with respect t_1 . Peak of the optimal properties

The value α correspond to the t_1 value that we should use to maximize the stiffness and damping at the same time. Being accurate is a must to achieve this peak due to we can get the maximum optimal properties very close to the unstable area.

3.13. Real world applications

The original intention of using negative stiffness in composite materials is to obtain high damping and high stiffness simultaneously, which has important applications in vibration isolation as required in earthquake engineering, high-speed trains, semiconductor factories and car bumpers. In our case, elasticity can be modified with the electric field and these composites may be used in high-performance sensor and actuators.

In addition, as we saw in the previous section we need to be accurate to maximize the stiffness and damping at the same time in a stable system, but using a capacitor in a small scale range could be a solution to achieve it.



3.14.Future work

Having done all the study of the viscoelastic system, we propose to create a system to verify its electromechanical function on a real system.

In the next illustration it's shown the basic functionality of the system made by Silicon. The Parallel plates will interact with electrostatic field, being attract to each edge acting as negative stiffness, while the shape of the system keeps the parallel plates in its position in order to stabilize it.

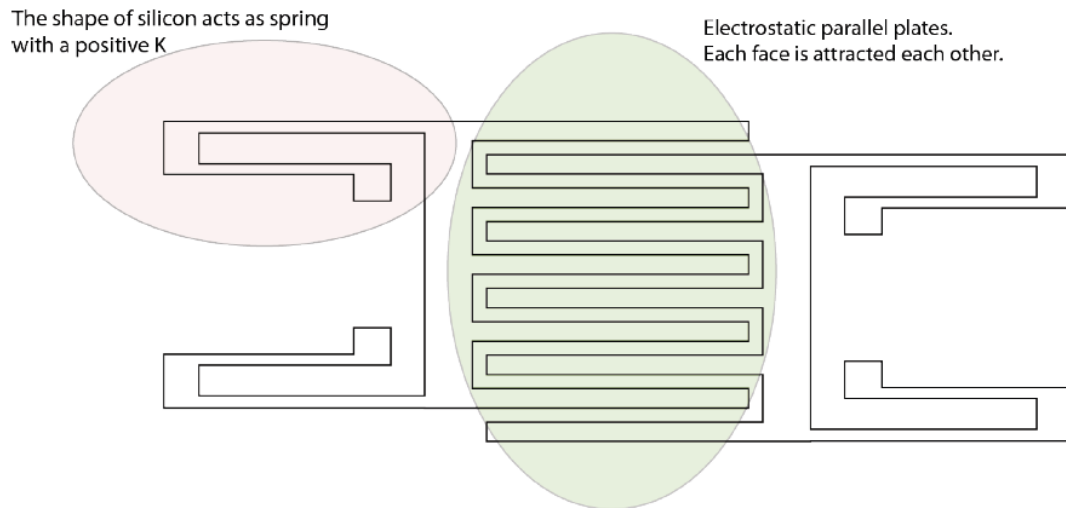


Figure 45: Sketch of a possible real model

This is a sketch about how to build it up as MEMS, but the dimensions and geometry need to be calculated conscientiously to avoid instability problems.

The next step would be to calculate a simulation of this system with a finite element program as COMSOL or Coventor and analyze the results of it.



3.15. Conclusions

Negative stiffness is unstable. However, it can be stabilized by positive-stiffness neighborhood. The extreme properties that we can achieve using negative stiffness elements can be very useful in future applications. But there are still many open questions in the field to be clarified.

In this second part of this project we could analyze a viscoelastic mechanic system with a negative stiffness element. After a rigorous mathematical study we conclude that it's possible to increase the stiffness and damping of a viscoelastic system including a negative stiffness element.

This opens the possibility to manufacture materials that adopt the mathematical conditions in order to increase mechanical properties.



4. Acknowledgments

I would like to express the deepest gratitude and appreciation to family, friends and Professor Lorenzo Valdevit for his guidance and persistent support.

In addition, I would like to thank all the members in my laboratory at the University of California, Irvine, for the good work environment created and especially, to Anna Torrents and Victor Arribas who have always helped and supported me.



5. References

- [1] Yun-Che Wang and Roderic S. Lakes, "Stable extremely-high-damping discrete viscoelastic systems due to negative stiffness elements" *Applied Physics Letters* Volume 84, Number 22
- [2] <http://physicsworld.com/cws/article/news/33127>
- [3] Lorenzo Valdevit, Alan J. Jacobsen, Julia R. Greer and Bill B. Carter, "Protocols for the optimal design of multi-functional structures: from hypersonics to micro-architected materials"
- [4] A. J. Jacobsen, W. Barvosa-Carter, and S. Nutt, "Micro-scale truss structures formed from self-propagating photopolymer waveguides," *Advanced Materials*, **19**[22] (2007).
- [5] A. G. Evans, M.Y. He, V. S. Deshpande, J. W. Hutchinson, A. J. Jacobsen, and W. B. Carter, "Concepts for enhanced energy absorption using hollow micro-lattices," *International Journal of Impact Engineering*, **39**[9] 947-59 (2010).
- [6] http://www.polytec.com/fileadmin/user_uploads/Products/Vibrometers/MSA-500/Documents/OM_BR_MSA-500_2010_05_E.pdf
- [7] <http://web.cecs.pdx.edu/~gerry/nmm/course/slides/ch09Slides.pdf>
- [8] R. S. Lakes, *Viscoelastic Materials*, Cambridge University Press 2009
- [9] A. Torrents, K. Azgin, S. W. Godfrey, E. S. Topalli, T. Akin, and L. Valdevit, "MEMS resonant load cells for micro-mechanical test frames: feasibility study and optimal design" *Journal of Micromechanics and Microengineering*, 20 (2010) 125004 (17pp)



[10] Hurwitz, A. (1964). "On the conditions under which an equation has only roots with negative real parts". Selected Papers on Mathematical Trends in Control Theory.

[11] H.J. Pain, The physics of vibrations and waves, Sixth Edition

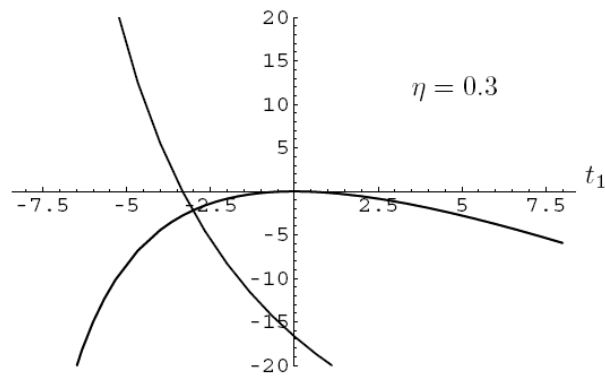


6. Annex: Mathematica[®] code

This annex contains the code used to perform some of the graphics of this project.

Mathematica software was used to plot these graphics.

Graphic 1:



Mathematica code for the graphic 1:

(* Parameters *)

$\omega = 1$

$\eta = 0.3$ (* eta value can be modified to see the effect produced to the derivate value on the instability point *)

$m = 10^{-12}$

$k = 10$

$P = 1$

$t_2 = 5$

(* A system matrix using t1 as a variable *)



```
AA[t1_]:={{0,1,0},{-k/m,0,-1/m},{t1 t2/eta,t1,-(t1+t2)/eta}}
```

(* Eigenvalues are calculated as a function of t1 variable *)

```
eig[t1_]:=Eigenvalues[AA[t1]]//Chop
```

(* The following expressions give us the real part of the eigenvalues *)

```
vp1[t1_]:=Re[eig[t1][[1]]]
```

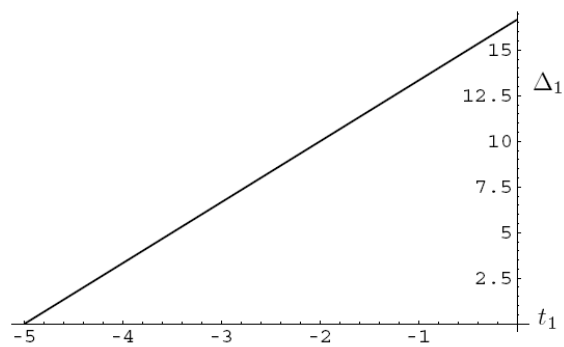
```
vp2[t1_]:=Re[eig[t1][[2]]]
```

```
vp3[t1_]:=Re[eig[t1][[3]]]
```

(* Graphic plot of the real part of the eigenvalues *)

```
Plot[{vp1[t1],vp2[t1],vp3[t1]},{t1,-8,8},PlotRange->{-20,20}]
```

Graphic 2



Mathematica code of graphic 2:

(* Parameters *)

```
omega=1
```

```
eta=0.3
```

```
m=10^-12
```

```
k=10
```

```
P=1
```

```
t2=5
```



(* A system matrix using t_1 as a variable *)

$AA[t_1] := \{(0, 1, 0), \{-k/m, 0, -1/m\}, \{t_1 \cdot t_2/\eta, t_1, -(t_1 + t_2)/\eta\}\}$

(* Characteristic polynomial of A matrix using t_1 as a variable *)

$Pol[t_1] := \text{CharacteristicPolynomial}[AA[t_1], x] // \text{Simplify}$

(* Coefficients of the characteristic polynomial with negative sign *)

$a0[t_1] := \text{Coefficient}[Pol[t_1], x, 3]$

$a1[t_1] := \text{Coefficient}[Pol[t_1], x, 2]$

$a2[t_1] := \text{Coefficient}[Pol[t_1], x, 1]$

$a3[t_1] := \text{Coefficient}[Pol[t_1], x, 0]$

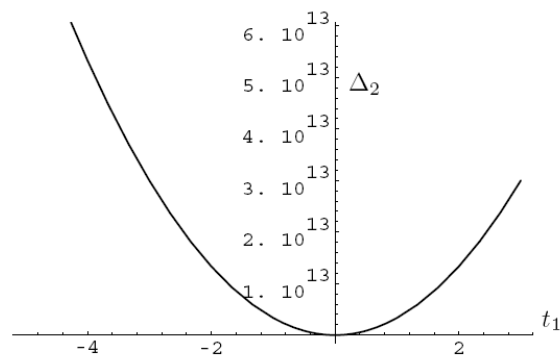
(* Δ_1 is the first coefficient in the Hurwitz criterion *)

$\Delta_1[t_1] := a1[t_1]$

(* Plot graphic of Δ_1 as a function of t_1 variable *)

$\text{Plot}[\{\Delta_1[t_1]\}, \{t_1, -5, 0\}]$

Graphic 3



Mathematica code of graphic 3

(* Parameters *)

$\omega = 1$

$\eta = 0.3$

$m = 10^{-12}$



k=10

P=1

t2=5

(* A system matrix using t1 as a variable *)

AA[t1_]:=({0,1,0},{-k/m,0,-1/m},{t1 t2/eta,t1,-(t1+t2)/eta})

(* Characteristic polynomial of A matrix using t1 as a variable *)

Pol[t1_]:=CharacteristicPolynomial[AA[t1],x]//Simplify

(* Coefficients of the characteristic polynomial with negative sign *)

a0[t1_]:=Coefficient[Pol[t1],x,3]

a1[t1_]:=Coefficient[Pol[t1],x,2]

a2[t1_]:=Coefficient[Pol[t1],x,1]

a3[t1_]:=Coefficient[Pol[t1],x,0]

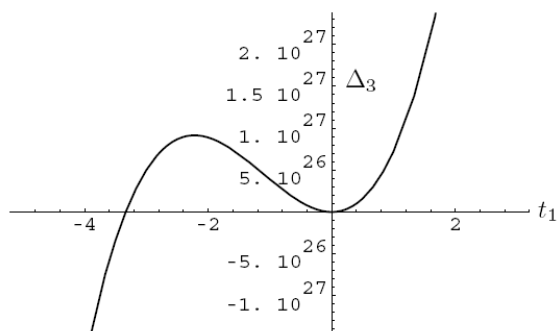
(* Delta2 is the second coefficient in the Hurwitz criterion *)

Delta2[t1_]:=Det[{{a1[t1],a3[t1]},{a0[t1],a2[t1]}}]

(* Plot graphic of Delta2 as a function of t1 variable *)

Plot[{Delta2[t1]},{t1,-5,3}]

Graphic 4



Mathematica code of the graphic 4

```
(* Parameters *)

omeg=1

eta=0.3

m=10^-12

k=10

P=1

t2=5

(* A system matrix using t1 as a variable *)

AA[t1_]:=({0,1,0},{-k/m,0,-1/m},{t1 t2/eta,t1,-(t1+t2)/eta})

(* Characteristic polynomial of A matrix using t1 as a variable *)

Pol[t1_]:=CharacteristicPolynomial[AA[t1],x]/Simplify

(* Coefficients of the characteristic polynomial with negative sign *)

a0[t1_]:=Coefficient[Pol[t1],x,3]

a1[t1_]:=Coefficient[Pol[t1],x,2]

a2[t1_]:=Coefficient[Pol[t1],x,1]

a3[t1_]:=Coefficient[Pol[t1],x,0]

(* Hurwitz matrix *)

HH[t1_]:=({a1[t1],a3[t1],0},{a0[t1],a2[t1],0},{0,a1[t1],a3[t1]})

(* Delta3 is the third coefficient in the Hurwitz criterion *)

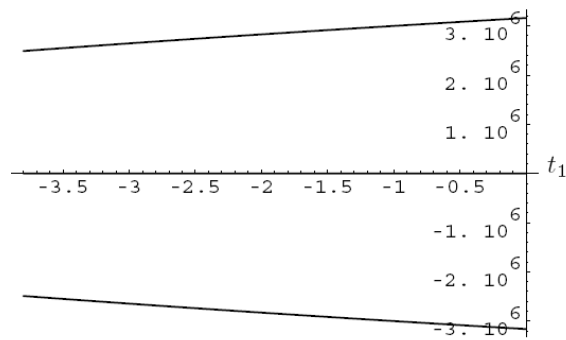
Delta3[t1_]:=Det[HH[t1]]

(* Plot graphic of Delta3 as a function of t1 variable *)

Plot[{Delta3[t1]},{t1,-5,3}]
```



Graphic 5:



Mathematica code of the graphic 5:

```
(* Parameters *)

omega=1

eta=0.3

m=10^-12

k=10

P=1

t2=5

(* A system matrix using t1 as a variable *)

AA[t1_]:={0,1,0},{-k/m,0,-1/m},{t1 t2/eta,t1,-(t1+t2)/eta}

(* Eigenvalues are calculated as a function of t1 variable *)

eig[t1_]:=Eigenvalues[AA[t1]]//Chop

(* The following expressions give us the imaginary part of the eigenvalues *)

vp1i[t1_]:=Im[eig[t1]][[1]]

vp2i[t1_]:=Im[eig[t1]][[2]]

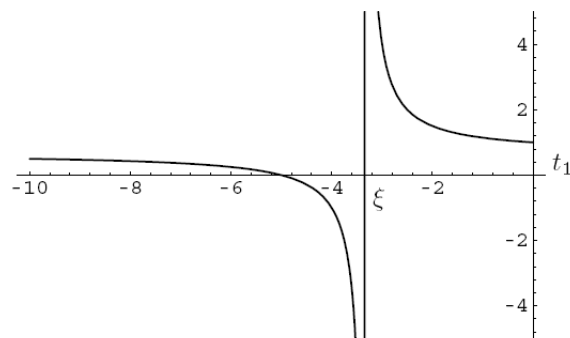
vp3i[t1_]:=Im[eig[t1]][[3]]
```



(* Graphic plot of the imaginary part of the eigenvalues *)

```
Plot[{vp1i[t1],vp2i[t1],vp3i[t1]}, {t1,-3.8,0}]
```

Graphic 6:



Mathematica code of graphic 6:

(* Parameters *)

```
omeg=1
```

```
eta=0.3
```

```
m=10^-12
```

```
k=10
```

```
P=1
```

```
t2=5
```

(* A system matrix using t1 as a variable *)

```
AA[t1_]:={{0,1,0},{-k/m,0,-1/m},{t1 t2/eta,t1,-(t1+t2)/eta}}
```

(* Vector of the equilibrium position of the system *)

```
ves[t1_]:=Inverse[AA[t1]].{0,P/m,0}
```



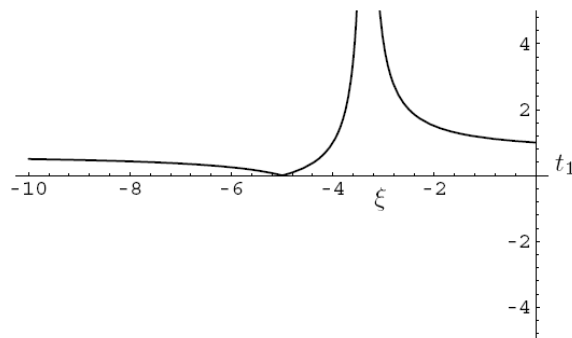
(* First component of the equilibrium position vector, it is equivalent to the displacement of the system *)

```
ue[t1_]:=ves[t1][[1]]
```

(* Plot graphic of the equilibrium position as a function of t1 *)

```
Plot[ue[t1] k, {t1, -10, 0}, PlotRange -> {-5, 5}]
```

Graphic 7:



Mathematica code of graphic 7:

(* Parameters *)

```
omega=1
```

```
eta=0.3
```

```
m=10^-12
```

```
k=10
```

```
P=1
```

```
t2=5
```

(* A system matrix using t1 as a variable *)

```
AA[t1_]:={0,1,0},{-k/m,0,-1/m},{t1 t2/eta,t1,-(t1+t2)/eta}
```

(* Vector of the equilibrium position of the system *)

```
ves[t1_]:=Inverse[AA[t1]].{0,P/m,0}
```



(* First component of the equilibrium position vector, it is equivalent to the displacement of the system *)

```
ue[t1_] := ves[t1] [[1]]
```

(* Plot graphic of the equilibrium position as a function of t1 *)

```
Plot[Abs[ue[t1]] k, {t1, -10, 0}, PlotRange -> {-5, 5}]
```

